One-dimensional silicone nanofilaments

Artus, Georg R J ; Seeger, Stefan

Abstract: A decade ago one-dimensional silicone nanofilaments (1D-SNF) such as fibres and wires were described for the first time. Since then, the exploration of 1D-SNF has led to remarkable advancements with respect to material science and surface science: one-, two- and three-dimensional nanostructures of silicone were unknown before. The discovery of silicone nanostructures marks a turning point in the research on the silicone material at the nanoscale. Coatings made of 1D-SNF are among the most superhydrophobic surfaces known today. They are free of fluorine, can be applied to a large range of technologically important materials and their properties can be modified chemically. This opens the way to many interesting applications such as water harvesting, superoleophobicity, separation of oil and water, patterned wettability and storage and manipulation of data on a surface. Because of their high surface area, coatings consisting of 1D-SNF are used for protein adsorption experiments and as carrier systems for catalytically active nanopartides. This paper reviews the current knowledge relating to the broad development of 1D-SNF technologies. Common preparation and coating techniques are presented along with a comparison and discussion of the published coating parameters to provide an insight on how these affect the topography of the 1D-SNF or coating. The proposed mechanisms of growth are presented, and their potentials and shortcomings are discussed. We introduce all explored applications and finally identify future prospects and potentials of 1D-SNF with respect to applications in material science and surface science.

DOI: https://doi.org/10.1016/j.cis.2014.03.007

Originally published at:
Artus, Georg R J; Seeger, Stefan (2014). One-dimensional silicone nanofilaments. Advances in colloid and interface science, 209:144-162.
DOI: https://doi.org/10.1016/j.cis.2014.03.007

One-Dimensional Silicone Nanofilaments

Georg R. J. Artus, Stefan Seeger*

Institute of Physical Chemistry, University of Zurich, Winterthurerstrasse 190, 8057 Zurich, Switzerland. Fax: +41 44 635 6813; Tel: +41 44 635 4450; E-mail: sseeger@pci.uzh.ch

Abstract

A decade ago one-dimensional silicone nanofilaments (1D-SNF) such as fibres and wires were described for the first time. Since then, the exploration of 1D-SNF has led to remarkable advancements with respect to material science and surface science: one-, two- and three-dimensional nanostructures of silicone were unknown before. The discovery of silicone nanostructures marks a turning point in the research on the silicone material at the nanoscale. Coatings made of 1D-SNF are among the most superhydrophobic surfaces known today. They are free of fluorine, can be applied to a large range of technologically important materials and their properties can be modified chemically. This opens the way to many interesting applications such as water harvesting, superoleophobicity, separation of oil and water, patterned wettability and storage and manipulation of data on a surface. Because of their high surface area, coatings consisting of 1D-SNF are used for protein adsorption experiments and as carrier systems for catalytically active nanoparticles.

This paper reviews the current knowledge relating to the broad development of 1D-SNF technologies. Common preparation and coating techniques are presented along with a comparison and discussion of the published coating parameters to provide an insight on how these affect the topography of the 1D-SNF or coating. The proposed mechanisms of growth are presented, and their potentials and shortcomings are discussed. We introduce all explored

applications and finally identify future prospects and potentials of 1D-SNF with respect to applications in material science and surface science.

Keywords

Silicone, polysiloxane, nanostructure, coating, one-dimensional, superhydrophobic

Graphical Abstract

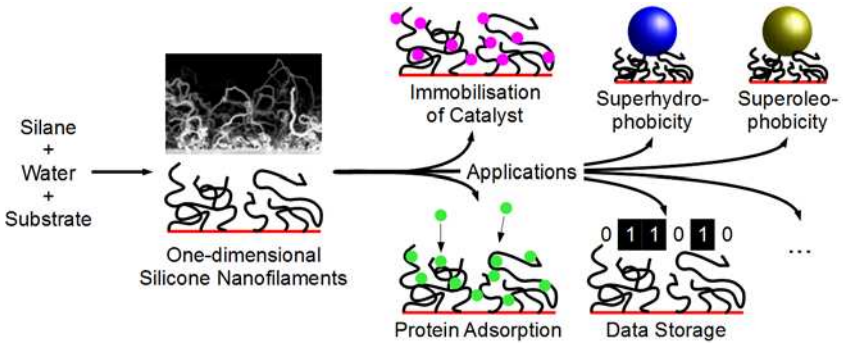

Highlights

- Comprehensive review of one-dimensional silicone nanostructures and coatings

- Chemical, optical, mechanical and wetting properties of nanostructures and coatings

- Comparison and discussion of coating parameters and their effect on the coating

- Presentation and discussion of suggested mechanisms of growth

- Introduction of explored applications

Contents

1. List of Abbreviations

1D-SNF One-dimensional silicone nanofilaments (including rods, tubes and fibres)

LPEI	linear polyethylenimine
MTES	Methyltriethoxysilane
MTMS	Methyltrimethoxysilane
ODS	Octadecylsilane
OTS	Octyltrichlorosilane
PDMS	Polydimethylsiloxane
PFDTS	1*H*,1*H*,2*H*,2*H*-Perfluorodecyltrichlorosilane
PFOTS	1*H*,1*H*,2*H*,2*H*-Perfluorooctyltrichlorosilane
TCES	Trichloroethylsilane
TCMS	Trichloromethylsilane
TCS	Tetrachlorosilane
TFPTCS	3,3,3-Trifluoropropyltrichlorosilane
TMCS	Trimethylchlorosilane
VTS	Vinyltrichlorosilane

2. Introduction

Silicones, also called polysiloxanes, belong to one of the most important classes of chemical compounds discovered in the last century. Whereas the name ‘silicone’ dates back to 1901, it was the Müller–Rochow synthesis of organochlorosilanes—the starting material for silicone chemistry—which set the basis for industrial production beginning in the 1940s [1, 2]. The unique chemical and physical characteristics of silicones, e.g. chemical inertness, oxidative stability, dielectric and thermal properties, made them an indispensable material class being found as resins, elastomers, oils, gels, sealants, electrical insulators, antifoaming agents and hydraulic media [3, 4].

In spite of the widespread use of silicones, little is known about this material at the nanoscale. Spherical colloidal particles have been known for more than 40 years [5], but template-free one-dimensional nanoparticles such as filaments, wires, tubes and fibres were discovered only

in this century [6, 7]. With diameters of several tens of nanometres and maximum lengths approaching the millimetre scale, these 1D-SNF exhibit a remarkable aspect ratio on the order of 10000. They may be grown onto a substrate either from a solution or via a gas-phase deposition process [8–10]. The high density of 1D-SNF leads to a coating on the substrate. Probably, the most outstanding property of these coatings is their extreme water repellency [7–9, 11–14] with contact angles up to 180° being measured [7]. Therefore, the investigation of the superhydrophobicity of 1D-SNF coatings either aiming at commercial applications or with respect to the theoretical understanding is the central part of many studies [6–30]. This is due to the facts that (1) many technologically important materials such as glass, silicon, textiles or polymers can be coated, (2) the coating is transparent perfectly, (3) it is free of environmentally questionable fluorine [31, 32] and (4) the gas-phase or solution-phase deposition techniques allow the coating of complex-shaped substrates that may be required for a potential application. The formation of a plastron can be used for the storage and manipulation of binary data on a superhydrophobic surface [33]. By chemical modification, switchable wettability can be achieved [29] or the coating can be further tuned from superhydrophilic to superoleophobic or combinations. This leads to further interesting applications such as highly oil-repellent coatings [24, 34, 35], substrates with patterned wettability or wettability gradients [35–39] or materials for the separation of oil and water [40]. A coating comprised of 1D-SNF is highly porous. The high internal surface area has been exploited for protein adsorption experiments and for the immobilisation of a catalyst [41–43].

Besides these already explored applications, many more utilisations of 1D-SNF can be envisioned. One-dimensional particles are used to modify the properties of a matrix material, as highly sensitive gas and biosensors and for hydrogen storage or catalysis. They can self-assemble to form new hierarchical structures on surfaces and they have found numerous applications in the fields of nano-optics and nanoelectronics [44–51]. One-dimensional

particles are the lowest dimensional particles for studying transport phenomena at the nanoscale, such as conduction of heat or electrical current, and they are the simplest mechanical, electrical or thermal interconnectors. Therefore, all types of one-dimensional nanoparticles will belong to the basic constituents of future nanodevices. Here 1D-SNF may play a special role for several reasons: (1) 1D-SNF can be synthesised at room temperature. In contrast, syntheses of most one-dimensional nanoparticles require high temperatures potentially restricting their implementation in complex nanodevices. (2) 1D-SNF consist of soft matter. This again is in contrast to other one-dimensional particles, which often consist of hard matter, e.g. metals or metal oxides [52]. (3) Silicones consist of the highly abundant and therefore comparably cheap elements hydrogen, carbon, oxygen and silicon. (4) Silicones offer highly desirable characteristics, e.g. viscoelastic properties or thermal and chemical stability. Their inertness with respect to environmental and health issues is of special interest to nanotechnology.

The discovery of 1D-SNF opened a very interesting field of research at the interface of surface science, silicone chemistry and nanotechnology. With respect to the great potential for applications and future scientific research we summarised the current knowledge about 1D-SNF in this review.

3. Synthesis

3.1. General aspects

The basic chemistry behind the formation of 1D-SNF corresponds to the synthesis of polysiloxanes. The overall reaction for all syntheses summarised in this chapter can be formally subdivided into two steps: (1) hydrolysation of all hydrolysable groups X of the starting silane forming a trisilanol (equation 1) and (2) subsequent condensation (equation 2) yielding a polysilsesquioxane. The exact sequence and kinetics of all possible hydrolysis and condensation reactions are unclear, e.g. homo and heterofunctional condensation may occur

[53]. The overall reaction assuming complete condensation for simplicity is given in equation 3.

$$n\ RSiX_3 + 3n\ H_2O \rightarrow n\ RSi(OH)_3 + 3n\ HX \quad (1)$$

$$n\ RSi(OH)_3 \rightarrow [RSiO_{3/2}]_n + 3n/2\ H_2O \quad (2)$$

$$n\ RSiX_3 + 3n/2\ H_2O \rightarrow [RSiO_{3/2}]_n + 3n\ HX \quad (3)$$

Hydride, chloride or alkoxide is used as the hydrolysable group X yielding molecular hydrogen, hydrochloric acid or an alcohol as byproduct HX, respectively. R is an organic residue, mainly vinyl or methyl groups are used. There is evidence that complete condensation of all the hydroxyl groups of the silanol does not occur [11] as observed for silicone resins in general [54]. Assuming complete hydrolysis of the chlorosilane, the polysiloxane will have the general formula $[RSiO_x(OH)_{3-2x}]_n$ with $0 < x < 3/2$.

Besides the mere chemical reactions, additional physico–chemical mechanisms are suggested to cause the formation of one-dimensional structures. These mechanisms are summarised in chapter 3.8.

The known synthesis methods of 1D-SNF can be divided into two main groups: synthesis in the gas phase or in a solvent. Coatings in the gas phase are conducted by chemical vapour deposition onto a substrate. In the case of solvent deposition, the coating of a substrate or synthesis of 1D-SNF with embedded gold nanoparticles can be distinguished.

Coated substrate materials include fabrics made of cotton [8, 13, 14, 30, 55], wool [8, 14], silk [14], viscose [14], cellulose acetate [14], polyacrylnitrile [14], polyester [14, 40], Kevlar® [22], wood [8], polyethylene [8], silicone [8], ceramics [8], glass [8, 11, 12, 18, 19, 24, 28, 29, 35, 36, 41, 43, 56, 57], quartz or silica [16, 57], silicon [7–10, 12, 16, 42, 58–62], germanium [16], titanium [8, 9] and aluminium [8, 16, 63] (figure 1).

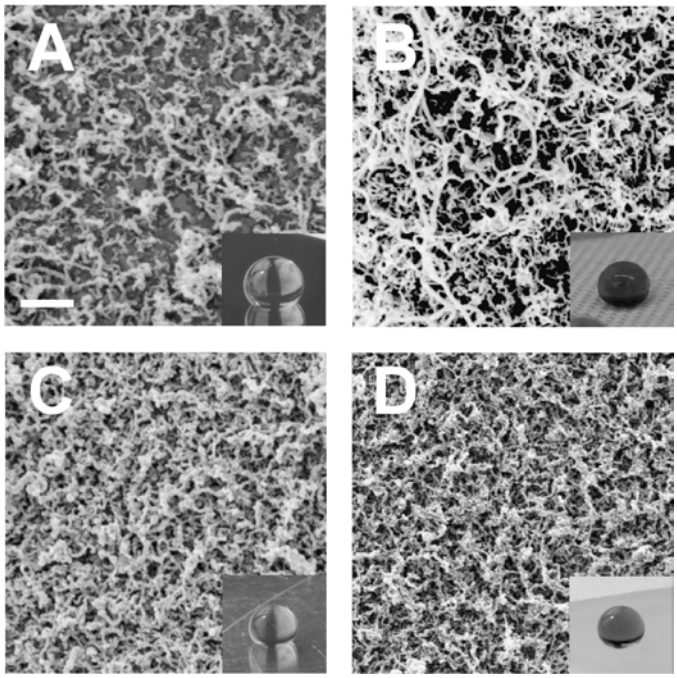

Figure 1. EM images of the 1D-SNF coatings on silicon (A), cotton (B), aluminium (C) and PDMS (D). The white bar corresponds to 200 nm. The inset photographs show drops of water on the respective surfaces. Adapted from [39] with permission. Copyright 2008, Taylor & Francis.

3.2. Surface activation

There is consensus in all published studies that hydroxyl groups need to be present on the surfaces to be coated and therefore, most substrates need cleaning and activation prior to coating to produce hydroxyl groups on the surface. This is performed in solvents, alkaline or cleansing solutions with or without ultrasonication [8, 11, 13, 16, 18, 24, 41, 43, 56, 63], activation in a plasma using oxygen [7–10, 16, 36, 57, 59] or a mixture of oxygen and hydrogen as process gas [60–62], treatment in strongly oxidising liquids such as a piranha solution [16, 28, 29], ozone in combination with UV-light [64], or combinations of these methods [12, 60–62, 64]. Fabrics may be subjected to a specific procedure [30].

3.3. Synthesis in the gas phase

All procedures described for coating in the gas phase are similar. Most of the coatings are conducted at room temperature in a coating atmosphere of air at normal pressure [6, 8, 9]. Also, an argon atmosphere at a pressure of 167 mbar [10, 16, 22] or pure gaseous water and silane are used [60–62]. The necessary amount of water in the reaction chamber is adjusted using residual surface-adsorbed water [10], flushing the volume with humidified gas [8], evaporation of predefined volumes of water [16], aqueous sodium chloride solutions [9] or by exploiting the water naturally absorbed by cotton [30]. The humidity values ranged from 10% to saturation but optimum values are reported to range between 25% and 50% [8, 9]. The reaction is initiated by evaporation of the volatile silanes into the reaction chamber [8, 10, 16] or by introducing the substrate into the coating atmosphere [9]. The following silanes have been used: mostly TCMS, but also pure VTS or VTS and TFPTCS consecutively [10, 16], a mixture (7.9 / 92.1 mol/mol) of TCMS and MTMS [14], TCES [56] or an azeotropic mixture (52.6 / 47.4 mol/mol) of TMCS and TCS [9]. 1D-SNF are observed to grow within minutes, although longer reaction periods are often applied. The samples may be annealed at temperatures above 100 °C subsequent to synthesis [8, 9, 16, 28, 30, 63]. Nouri et al. observed improved superhydrophobicity after radiative heating compared to convective heating [63].

The upper part of table 1 summarises the coating parameters for gas-phase coating procedures published to date. A graphical presentation is given in figure 2.

Ref.	Silane(s) (molar ratio)	Substrate	c_S / mM	c_W / mM	Molar ratio silane / water	Water saturation / %[a]
Gas-phase coatings						
[9]	TMCS/TCS 52.7 / 47.7	Si	-	0.46	-	43
[21]	TCMS	glass	0.08	0.36	0.23	33
[14]	MTMS/TCMS 92.1 / 7.9	different textiles	0.33	0.43–0.54	0.61–0.77	40–50
[8]	TCMS	glass	0.39	0.39	1.00	37
[56][b]	TCES	glass	0.45	0.71	0.63	62

[40]	TCMS	polyester	0.52	0.38–0.7	0.75–1.39	35–65
[10, 16]	VTS	Si	0.63	1.14	0.56	100
[59]	TCMS	Si	0.85	0.32	2.64	30
Solvent-phase coatings						
[38]	TCMS	glass	0.84	3.8	0.22	14
[38]	TCMS	glass	3.4	7.6	0.45	29
[24]	TCMS	glass	5.33	8.02	0.66	31
[56][b]	MTES	glass	8.4	9.9±2.4[c]	0.84±0.2[c]	38±10[c]
[29]	TCMS	glass	10.6	8.3	1.28	32
[15]	TCMS	glass	10.6	21.1	0.5	80
[12]	TCMS	glass	14	(~16)[d]	(~0.9)[d]	60
[28, 64]	TCMS	glass	80	1000 (~26)[e]	0.08 (~3.1)[e]	>100[e]
[13]	TCMS	cotton	100	(~13)[d]	(~7.7)[d]	40–50
[11]	MTMS	glass	180	118 (~37)[f]	1.53 (~4.9)[f]	>100[f]
[7, 58]	TCMS	Si	1000	(~13)[d]	(~80)[d]	30–65

Table 1. Summary of all coating conditions reported to date sorted by increasing concentration of silane. Identical conditions used in follow-up publications are not listed. For better comparison, all concentrations are converted to units of millimoles per litre. c_S = concentration of silane, c_W = concentration of water. The values in brackets are estimated as indicated. a) Corresponds to relative humidity in the gas phase or percentage of the saturation concentration of water in the corresponding solvent. b) Synthesis of nanotubes. c) Dispersion of an unknown but limited amount of aqueous hydrochloric acid in moist toluene. Thus, the true values range between the computed limits. d) Only the relative humidity of air in contact with the solvent is reported (range 30%–65%). Thus, the actual concentration of water can be estimated to be on the order of ~50% of the saturation concentration of water in toluene (~13 mM [65]). e) Dispersion of excess aqueous hydrochloric acid in toluene as a solvent. Thus, the actual concentration of dissolved water can be estimated to be on the order of the saturation concentration in toluene (~26 mM [65]). f) Dispersion of excess aqueous hydrochloric acid in petrol ether as a solvent. Thus, the actual concentration of dissolved water can be estimated to be on the order of the saturation concentration in hexane (~37 mM [66]).

It should be mentioned that very similar syntheses were already conducted by Patnode in 1940 [67] where the related patent describes a vapour-phase reaction of pure organo-silicon halides or mixtures thereof with emphasis on TCMS. A similar reaction using the azeotropic mixture of TMCS and TCS was patented by Norton in 1946 [68]. Both coating methods resulted in coated substrates with pronounced water repellency. From this, it is reasonable to assume that 1D-SNF were formed. Of course, proving the existence of one-dimensional nanoparticles was impossible at that time.

Vinyltrimethoxysilane, hexyltrichlorosilane and 5-hexenyltrichlorosilane have been tested as educts by Rollings and Veinot, but here no 1D-SNF were formed as observed by EM [16]. The reasons were assumed to be lower reactivity of the alkoxysilanes or greater hydrophobicity of longer hydrocarbon chains.

3.4. Synthesis in solvent

3.4.1. Coating of a substrate

All coating protocols are based on those reported by Zimmermann et al. and Gao and McCarthy, who used TCMS as the precursor in toluene [6, 7, 23, 38, 39, 58]. The substrates, preferably silicon wafers or glass, were immersed in dry toluene in a reaction chamber. Water was introduced by exposure to air with a relative humidity between 30% and 65%. The silane was added to a final concentration of 1 mM [38, 39] or 1 M [7, 58]. The reported durations of reactions ranged from one to several hours. The samples were rinsed with toluene, ethanol and ethanol / water (1 / 1) [7, 58]. According to Gao and McCarthy, rinsing with ethanol induces a phase separation. The samples were dried at 120 °C for 10 min [7] or at 200 °C for hours [39].

Quite similar methods were applied by Jin et al. [15] and Wong et al. [28], where Jin et al. adjusted the water content by mixing dry and wet toluene. Wong et al. supplied an excess amount of water by adding 12 M aqueous HCl.

Shateri-Khalilabad reported the coating of a graphene-cotton sample using TCMS in *n*-hexane [55]. The coating was finished by washing with acetone-ammonia and water.

Chen et al. presented a route using MTMS or MTES as an educt in petrol ether as the solvent [11]. Water and an acid catalyst were introduced by dispersing hydrochloric acid (6 M in water) in the solvent via ultrasonication. After 1.5 h (2 h for the ethoxysilane), the substrates were rinsed with petrol ether, ethanol and water and finally dried in air. In a vapour solution variant of this method, the sample was immersed in a solution of silane in petrol ether in an open Petri dish. This dish was then exposed to the vapour phase of a 12 M aqueous hydrochloric acid solution.

1.1 mmol MTES in toluene in combination with concentrated HCl was also used by Stojanovic et al. for the growth of nanotubes [56].

The lower part of table 1 and figure 2 summarise the parameters employed for solvent coating procedures.

3.4.2. Synthesis of 1D-SNF with embedded gold nanoparticles

Prasad et al. reported the synthesis of non-surface bound one-dimensional polysiloxane nanostructures [69]. 10 µL of water were added to 3 mL butanone or 2-pentanone containing 12 mg of colloidal gold. After adding 300 mg of OTS, the mixture was refluxed for 90 min under an Ar atmosphere. Without water, no polymerisation was observed. The polymerisation was catalysed by gold-nanoparticles such that 1D-SNF were formed. Often, these 1D-SNF adopt a helical structure. A gold nanoparticle was included at the tip of each 1D-SNF.

Goyal et al. published a similar 1D-SNF synthesis at room temperature by the *in-situ* formation of gold particles from chloroauric acid [70].

3.5. Effect of coating conditions

The dependency of the properties of the final coating, e. g. hydrophobicity, thickness of the coating or optical transparency, on the coating conditions is very important for two reasons. On the one hand, knowledge of these dependencies allows optimising the coating with respect

to the desired application. On the other hand, understanding the impact of the conditions on the properties of the coating will offer insight into the mechanism of growth. Table 2 summarises reported variations of the concentration of silane, the concentration of water, the reaction time and the temperature and the observed effects on the coating. The applied concentrations of water are plotted against those of the silane in figure 2.

Ref.	Quantity varied / range	Impact	Conditions
	***c*W**		
[56]	0.37 – 0.82	$c_W = 0.37$: $d \approx 30$ nm $0.37 \leq c_W \leq 0.66$: tapered 1D-SNF in addition $0.66 \leq c_W \leq 0.74$: optimum, tapered 1D-SNF with cavity, $l \approx 12$ µm, SA < 1° $0.74 \leq c_W \leq 0.76$: tapered 1D-SNF and microtubes $c_W = 0.78$: microtubes $c_W \approx 0.82$: circular structures	glass, gas phase, c_S = 0.45, t = 12 h
[16]	0.91 – 1.36	$c_W = 0.91$: thin flat film, D < 20 nm $c_W = 1.11$: optimum, $d \approx 35$ nm, $l \approx 1$ µm $c_W = 1.36$: structured film, $D \approx 250$ nm	Si, gas phase, $c_S = 0.62$, t = 1 h
[38]	1.28 – 5	l and d increase with c_W $c_W > 2.84$: CA > 160°, SA < 5° $c_W > 3.8$ conglomeration of thicker filaments	glass, toluene, $c_S = 0.84$, t = 4 h
[24]	2.7 – 9.37	optical transmittance decreases with c_W $c_W = 8$: optimum, $D = 6$ µm, $d = 60$ nm, $l > 1$ µm $c_W \neq 8$: shorter and thinner 1D-SNF $2.7 \leq c_W \leq 9.37$: CA > 160°, SA < 6°	glass, toluene, $c_S = 5.33$, t = 6 h
[12]	7.9 – 23.8	$c_W = 7.9$: agglomeration of 1D-SNF $c_W = 15.8$: optimum, network of 1D-SNF, $d \approx 36$ nm $c_W = 23.8$: agglomeration of 1D-SNF $7.9 \leq c_W \leq 23.8$: CA > 155°, HY < 8°	glass, toluene, $c_S = 14$, t = 2 h
[15]	0 – 26.4	$c_W < 15.8$: nano-protuberances $c_W = 15.8$: few 1D-SNF $c_W = 21.1$: optimum, network, CA = 170.1° $c_W = 26.4$: nanospheres	glass, toluene, $c_S = 10.6$, t = 1 h
	***c*S**		
[56]	0.37 – 0.74	no discernible effect	glass, gas phase, c_W = 0.71, t = 12 h
[16]	0.47 – 1.6	$c_S = 0.47$: flat film $c_S = 0.62$: optimum, $d \approx 35$ nm, $l \approx 1$ µm $c_S = 0.79$: small and sparse 1D-SNF $c_S = 1.6$: rough film	Si, gas phase, $c_W = 1.1$, t = 1 h
[38]	0.16 – 6.8	formation of conglomerates with increasing c_S $0.16 \leq c_S \leq 0.68$: base layer of 1D-SNF, $d \approx 15$ nm, l > 100 nm, individual 1D-SNF with $d \approx 50$ nm, $l > 1$ µm in addition, CA > 150°, SA < 30°	glass, toluene, $c_W = 7.6$, t = 4 h

		c_S > 1.68: CA > 160°, SA < 5°	
[12]	7 – 500	c_S = 7: discrete 1D-SNF, $d \approx 49$ nm c_S = 14: optimum, quasi-network of 1D-SNF, $d \approx 36$ nm, CA = 168°, HY = 6° c_S = 50: quasi-network of 1D-SNF, $d \approx 76$ nm c_S > 50: discrete 1D-SNF, spherical particles	glass, toluene, $c_W \approx 16$, t = 2 h
[28]	20 – 100	c_S = 80: optimum, CA > 150°	glass, toluene, aqueous HCl, t = 5 h
[15]	2.1 – 500	c_S = 2.1: discrete submicron spheres c_S = 10.6: optimum, nanofibre network, CA = 170.1° $c_S \geq 106$: spherical particles	glass, toluene, c_W = 21.1, t = 1 h
[13]	10 – 1000	c_S = 10: film c_S = 50: short and thin 1D-SNF c_S = 100: optimum, cross-linked 1D-SNF, CA > 160°, SA < 20° $c_S \geq 500$: less filamentous but irregular structures	cotton, toluene, $c_W \approx 13$, t = 2 h
	t		
[9]	30 s – 10 min	l and CA increase with t t = 30 s: nucleation sites $t \geq 2$ min: CA = 176°, HY = 0° t = 10 min: D > 20 nm (ellipsometric)	Si, gas phase, c_W = 0.46
[16]	5 min – 1 h	l and CA increase with t t = 5 min: $l \approx 200$ nm t = 10 min: $l \approx 500$ nm t > 20 min: $l \approx 1$ µm	Si, gas phase, c_S = 0.62, c_W = 1.11
[12]	2 min – 2 h	l and CA increase with t t > 1 h: CA > 160°, HY < 10° t = 2 min: discrete 1D-SNF, D = 142 nm t > 2 min: increasing entanglement, transition to network, $d \approx 36$ nm t = 2 h: D = 321 nm	glass, toluene, c_S = 14, $c_W \approx$ 16
[56]	10 s – 12 h	l increases with t t = 10 s: base layer t = 3 min: holes in base layer t = 15 min: tubes, $l \leq 4$ µm t = 30 min: tubes, $l \approx 9$ µm t = 12 h: tapered 1D-SNF, $l \approx 12$ µm, SA < 1°	glass, gas phase, c_S = 0.45, c_W = 0.71
[38, 39]	1 h – 14 h	l and CA increase with t t = 1h: base layer of 1D-SNF, CA = 156°, SA = 60° t > 1h: longer 1D-SNF in addition t = 14h: CA = 167°, SA = 6°	glass, toluene, c_S = 0.84, c_W = 5.6
[28]	0.5 min – 6 h	CA increases with t t > 3h: CA ≈ 150°	glass, toluene, c_S = 80, aqueous HCl
[13]	2 min – 3 h	$t \leq 5$ min: nanoparticles, few tiny 1D-SNF, gain in mass by silane deposition 0.14 %min^{-1} 15 min $\leq t \leq$ 1200 min : l, d, frequency and entanglement of 1D-SNF increase with t t = 120 min: optimum, filamentous network, CA =	cellulose, toluene, c_S = 100, $c_W \approx 13$

		167°, SA = 33° t = 180 min: less 1D-SNF, particles and spheres, gain in mass by silane deposition < 0.01 %min^{-1}	
	T		
[28]	-22 °C – 60 °C	CA increases with T optical transmittance decreases with T	glass, toluene, c_S = 80, aqueous HCl, t = 5 h
[38]	10 °C – 50 °C	CA increases with T optical transmittance decreases with T	glass, toluene, c_S = 5.2, c_W = 6, t = 0.5 h

Table 2. Summary of all published variations of the coating conditions and resulting effects on the 1D-SNF coating. c_W = concentration of water, c_S = concentration of silane, t = reaction time, T = temperature, d = diameter of 1D-SNF, l = length of 1D-SNF, D = thickness of coating or layer, CA = contact angle, HY = contact angle hysteresis. All concentrations are computed to units of mM, the unit mM is omitted for brevity.

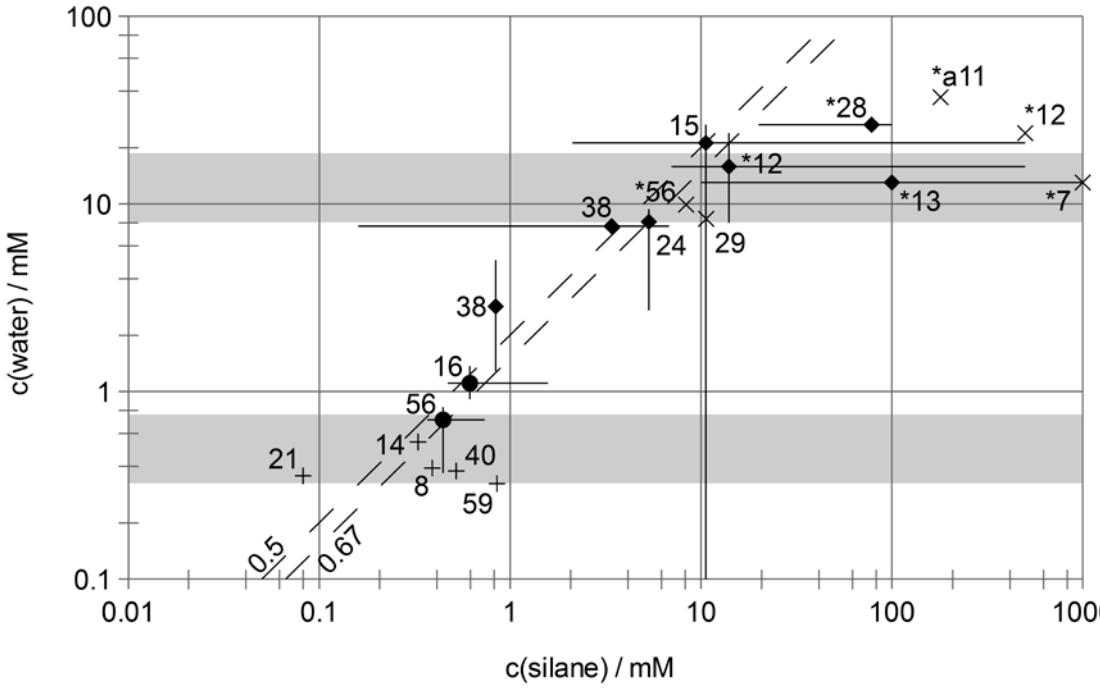

Figure 2. Log-log plot of applied concentrations of water and silane. Solid lines indicate the explored range of concentration. A filled symbol on a solid line marks the determined optimum (● gas phase, ♦ solvent). Conditions without optimisation are denoted by + (gas

phase) and × (solvent). The two dashed lines indicate the molar ratios water / silane of 0.67 and 0.5, respectively. The grey horizontal bars mark the range from 30% to 70% of water saturation in the gas phase (lower) and in toluene (upper). The numbers correspond to the references. *) the water concentration had to be estimated (compare table 1). a) petrol ether saturated with water was used instead of toluene. Thus, the upper grey bar does not apply.

In addition to the studies summarised above, Rollings and Veinot found that 1D-SNF are only formed when the substrate could equilibrate with the moist atmosphere prior to the release of silane [16]. It was concluded that an already existing water film of appropriate thickness on the substrate is necessary for filament formation. By varying the equilibration period subsequent to the release of silane, Rollings and Veinot concluded that the optimum growth of 1D-SNF can be achieved when the process is diffusion limited with respect to the transport of the silane to the substrate surface [16].

Rollings and Veinot also investigated the effect of the substrate material and the surface pre-treatment [16]. On surfaces activated in oxygen plasma or in piranha solution, the dense growth of 1D-SNF using VTS as a precursor was observed. Ultrasonication of the substrates in solvents resulted in a much less dense filament growth. Areas intentionally stained with OTS or TFPTCS remained uncoated. From this, it was concluded that hydroxyl groups at the surface are a prerequisite for the growth of 1D-SNF. On quartz and silica Rollings et al. found 1D-SNF with diameters between 50 and 70 nm and lengths between 5 and 10 µm. On silicon wafers, diameters were only around 35 nm with lengths ranging from a few hundred nanometres to around 1 µm [10, 16].

Zhang and Seeger reported quite similar observations [57]. After activation with oxygen plasma they found 1D-SNF of several micrometres in length and up to 70 nm in diameter on silica. On glass, which was activated and coated in the same batch as the silica, the 1D-SNF

were shorter than 500 nm and only up to 50 nm in diameter. Interestingly, without this activation, 1D-SNF selectively grew on glass but not on silica.

3.6. Scale up

Artus and Seeger presented a pilot plant for coating in the gas phase with TCMS [21] (figure 3). The casing was constructed from double-walled rib-reinforced polyvinylchloride. The size of the reaction chamber was of the size 1.88 m × 2 m × 2.2 m, allowing a maximum size for a flat sample of 1.3 m × 2 m. The chamber volume was 8.3 m^3, which corresponded to a scale-up factor of 1300 compared to the laboratory coating equipment. A ventilator for internal convection during coating and a wet scrubber running with 150 L of a sodium hydroxide solution for the absorption of acidic byproducts were integrated.

The necessary humidity ranged between 20% and 50% depending on the substrate material (as for the laboratory scale process). The amount of silane needed seemed to scale with the sample area to be coated. A typical coating was conducted with 80 mL of TCMS. 1D-SNF were observed already after 30 min, but contact angles were found to be superior after several hours of coating time. Analytical results of the characterisation of morphology, wettability and optical properties of the coating confirmed that similar 1D-SNF-coatings were obtained as on the laboratory scale. The successful coatings of large area glass panes, long glass tubes, square metres of polyester fabric and a polyester suit were reported.

Figure 3. Pilot plant with a volume of 8.3 m^3 for coating large area substrates. Adapted from [21] with permission. Copyright 2012, American Chemical Society.

3.7. Discussion of synthetic aspects

In the following section, we try to summarise and discuss the general aspects of the synthesis of 1D-SNF. The study of 1D-SNF with embedded gold nanoparticles presented by Prasad et al. is excluded because this synthesis fundamentally differs from 1D-SNF grown onto surfaces [69]. In addition, there is only one example of this type of synthesis.

The primary parameters expected to affect the growth of 1D-SNF onto surfaces are the concentrations of silane and water [1], concentration of the catalyst, temperature, pressure, whether the synthesis is conducted in a solvent or gas phase, absolute area and type of substrate and the pretreatment used. In addition, the chemistry of a surface is very sensitive to impurities, imperfections, irregularities and surface structures. Thus, for example, differences in the storage conditions, pretreatment, time of exposure to lab atmosphere, individual handling or specific characteristics of the coating equipment may induce different coating results, which are difficult to understand completely. Because of these exact effects often seemingly contrary or irreproducible results were obtained from investigations of the formation of alkoxysilane monolayers [73]. We note that the chemical growth of 1D-SNF on surfaces is closely related to the formation of two-dimensional silane monolayers and can be expected to be similarly complex. Thus, one can also expect different coating results from small differences in the coating protocols.

With respect to these uncertainties on the one hand and the large number of parameters involved in the synthesis of 1D-SNF on the other hand, only little data on the effects of the

[1] Concentrations are presented since the activities of the reactants are unknown. Especially it is unclear how the activities behave in a thin film of water on a surface. The example of aqueous hydrochloric acid, which is a constituent in the described systems, demonstrates the potential effect of replacing concentrations by activities: At a concentration of 5 mol kg^{-1} the activity of water dropped to 0.74 [71], whereas the activity coefficient of HCl increased to 2.38 [72].

coating parameters is published. Therefore, only a broad overview of the topic will be presented and discussed.

All published synthesis methods for 1D-SNF are quite similar in principle. All syntheses use educts of the type $RSiX_3$, where X is either an alkoxide or chloride. In one case, TCS was used in combination with TMCS [9]. All syntheses were reported to work at or close to room temperature. With few exceptions [16, 60–62], all syntheses were carried at normal pressure. The reaction conditions were maintained acidic throughout. Hydrochloric acid is either produced by the hydrolysation of chlorosilanes or it is added separately, and is certainly active as a catalyst. Syntheses of pure 1D-SNF under neutral or basic conditions have not been reported to date (compare chapter 7). In this respect, it is interesting to note that the polymerisation of silicic acid at acidic pH values allows chaining of nanometre-sized particles yielding one-dimensional structures, whereas this is not observed for a pH value above 7 [74]. It is also known that the condensation of silanols proceeds much faster under basic conditions compared to acidic environments [74, 75]. Presumably, a slow condensation reaction is a necessity for the formation of 1D-SNF. This makes sense in view of the fact that the formation of the one-dimensional structure must be caused by a physico–chemical self-assembly process (see chapter 3.8). Thus, one-dimensional growth can occur only when the condensation reaction is slower than the process of self-assembly.

The reported reaction times range from a few minutes [9, 12, 16] to several hours [8, 12, 21, 24, 28, 30, 56]. Here one has to distinguish between the growth of 1D-SNF and the optimum water repellency of the coating. The formation of short 1D-SNF (~100 nm) is already reported after few minutes, while longer reaction times led to longer 1D-SNF (figure 4). Some studies suggest that the length of the 1D-SNF increases fast initially but levels off at elongated reaction times [9, 13, 56]. The thickness of the coating grows correspondingly. The reasons for this type of kinetics are unclear. Time-dependent measurements of the concentrations of reactants are not reported. Since water and chlorosilanes can be expected to react everywhere

in the reaction vessel and not only on the substrate, the concentration of the educts should decline gradually. This would reduce the growth rate of 1D-SNF. It is also conceivable that slower diffusion processes dominate the kinetics at elongated reaction times, especially when low concentrations of silane and water are used or the reaction is conducted without convection.

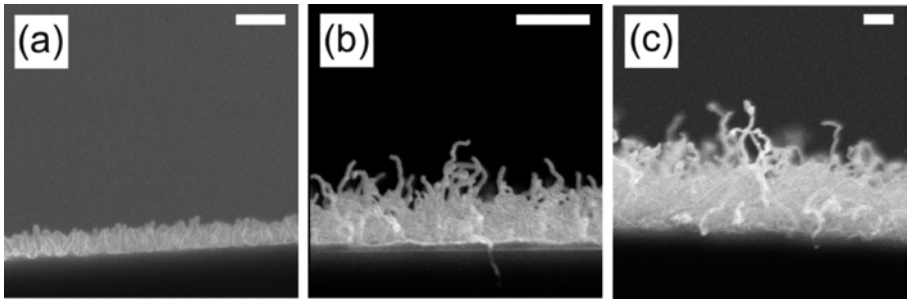

Figure 4. Cross-sectional SEM images demonstrating the increasing length of 1D-SNF with longer exposure times to VTS: a) 5 min, b) 10 min and c) >20 min. The scale bars correspond to 500 nm. Adapted from [16] with permission. Copyright 2008, American Chemical Society.

The current data on the dependency of the diameter of the 1D-SNF on the reaction time are too scarce to derive any correlation. However, radial growth over time seems to be improbable since tapered 1D-SNF should be observed in this case. Actually, constant diameters along the whole length of 1D-SNF seem to be most frequent (see chapter 5.1.1). One exception are tapered 1D-SNF made from TCES. However, also here radial growth was reported to be negligible compared to axial growth [56].

Virtually all studies reveal improved water repellency after elongated reaction times. An obvious explanation is that longer 1D-SNF imply a higher surface roughness which will enhance superhydrophobicity [76]. Improvement in the water-repellent properties without further growth of the filaments during additional reaction time can be understood in terms of condensation of the hitherto unreacted hydroxyl groups in the already formed or nearly finished filament. The presence of acid can accelerate this condensation by catalysing the

cleavage, formation and consequently reorientation of siloxane bonds. Thus, unreacted hydroxyl groups can become close enough together to condensate. The surface energy of the filament may be an additional driving force for the rearrangement of siloxane groups. In a non-polar and hydrophobic reaction environment, provided by gas or toluene, the orientation of methyl groups towards the environment and the orientation of polar hydroxyl groups towards the interior of the filament, where condensation may occur in addition, are favourable energetically. These processes in the final stage of filament formation would explain why the contact angles improve when the sample is left in the reaction environment. Likewise, contact angles do not improve for samples removed from the coating environment and stored under lab atmosphere [19]. Condensation of hydroxyl groups can also be facilitated by heating. This is consistent with the observation of improved water repellency and improved chemical stability after annealing the samples [8, 18, 63].

From the stoichiometry of the reaction, one can expect a ratio of silane / water in the range 0.5 to 0.67. A ratio of 0.67 corresponds to complete condensation and the formation of $[RSiO_{1.5}]_n$ while a ratio of 0.5 can be expected for the formation of $[RSiO(OH)]_n$ where only two of three hydroxyl groups per silicon atom condense on average. This order of magnitude is quite well reflected by the experimentally used ratios of educts for the majority of all syntheses. Importantly, this is especially true in cases where the amounts of silane or water were optimised, as it is illustrated in figure 2 (the two dashed lines mark the ratios 0.5 and 0.67) and also summarised in table 1. Deviations from this optimum ratio seem to appear in solution at higher silane concentrations. However, for all of these points the exact water concentration had to be estimated or an excess of water was used (see table 1). In the latter case, because of the low solubility of water in organic solvents, the absolute amounts of water present were higher than it is reflected by the saturation concentrations.

Studies on the variation in the water concentration have been performed by several researchers (chapter 3.5) [12, 15, 16, 24, 38, 56]. The consistent outcome of these experiments

is that at low water concentrations no or only short 1D-SNF grow, whereas at high concentrations, rough films, spheres or other non-fibrous structures are observed, sometimes in addition to filamentous structures. Ideally, medium water concentrations are used which is depicted in figure 2 (see also table 1). The two grey horizontal bars mark water concentrations between 30% and 70% of the saturation level in air and toluene. Most of the applied water concentrations fall in this medium range. This level of saturation determines the thickness of the adsorbed water layer on the substrate. This is a strong indication that an appropriate thickness of the water film on the substrate is necessary for the formation of 1D-SNF in general, as explicitly stated by Rollings and Veinot [16]. The relatively narrow range of useful water concentrations may also be reflected by the fact that the water concentrations vary only by a factor of ~3 for syntheses in the gas phase and by a factor of ~10 for syntheses in the solvent.

Table 1 shows that the concentrations of silane vary by approximately one order of magnitude in the gas phase and approximately three orders of magnitude in the solvent. From this, one can conclude that the amount of silane is not particularly limiting the growth of 1D-SNF, as it seems to be the case for water. It is noted that in the gas and in the liquid phase, the feasible silane concentrations are categorically higher than those for water for basic physico–chemical reasons: the saturation pressure of TCMS exceeds that of water at 22 °C by a factor of 8 [77, 78], and the solubility of TCMS in toluene is higher by a factor of at least 400 compared to water [65] [2]. Table 1 and figure 2 reveal that for some syntheses an excess of silane is applied (molar ratio silane / water > 2 0.67). In these cases, the chlorosilane can not be hydrolysed completely. Hydrolysation and potentially consequential condensation will take place subsequent to the actual reaction when the sample is exposed to the humidity of the normal atmosphere. The effects of this termination of the reaction on the morphology and wettability of the 1D-SNF are unexplored.

[2] The solubility of TCMS in toluene has not been determined to our knowledge. According to the applied concentrations, the saturation concentration is at least 1 M.

Most researchers reported an optimum concentration also for the silane [12, 13, 15, 16, 28]. Small silane concentrations produced silicone films, small spheres or only sparse and short filaments. At high concentrations, ball-like particles, conglomerates or agglomerates with more random topography are found. At the optimum concentration, the longest 1D-SNF, complex fibrous networks or the highest contact angles are observed (table 2) [12, 13, 15, 38]. It remains unclear whether a high silane concentration leads to longer and thicker structures *per se*, or whether the high concentration simply accelerates the growth of 1D-SNF because of kinetic reasons. Varying the reaction time revealed that longer and thicker 1D-SNF can be grown also at low silane concentrations albeit after extended duration [38, 39]. The little data on the dependency of the diameter of the 1D-SNF on the concentration of silane are ambiguous.

With respect to the concentrations or absolute amounts of educts, one would expect that the area of the substrate, the area of the chamber walls, which may or may not react in competition to the substrate, or the absolute volume of the coating chamber affect the required concentrations of educts. Beside an optimum ratio of silane / substrate area of 0.137 mmol cm^{-2}, as reported by Veinot et al. [22], no data illustrating such effects have been published to date. Coating in a pilot plant required the same intermediate levels of relative humidity compared to the lab-scale equipment, which was smaller in volume by a factor of 1300 [21]. This again indicates the importance of an adequate thickness of the adsorbed water layer on the substrate, which depends on the level of water saturation but not on the volume of the reaction vessel.

In two studies the reaction temperature was varied [28, 38]. Both report increasing contact angles but decreasing optical transparency with rising temperature.

3.8. Mechanism of 1D-SNF formation

The formation mechanism of 1D-SNF is an issue of high interest for various reasons. First, the 1D-SNF are quite a new class of nanoparticles. Second, 1D-SNF consist of soft matter,

which is a rarer case among all one-dimensional particles. Third, a hitherto unknown mechanism is likely since three of the four suggested mechanisms do not correspond to the classical and known mechanisms for growth of one-dimensional nanoparticles [44, 52].

3.8.1. Composition-based mechanism

Chen et al. presented studies of 1D-SNF characterised by thermogravimetry, differential thermal analysis and Fourier transform infrared spectroscopy (FT-IR) spectroscopy [11]. Analysis of the thermogravimetric results revealed a chemical formula $CH_3SiO_{1.12}(OH)_{0.76}$ for the final 1D-SNF. Because of kinetic and molecular weight considerations, it is concluded that the final product consists of the two building blocks $CH_3SiO_{1.5}$ and $CH_3SiO(OH)$ in a molar ratio of ~1 / 3. It is further concluded that under equilibrium conditions, every $CH_3SiO_{1.5}$ unit is connected to three $CH_3SiO(OH)$ units, resulting in secondary building units with three connectivity points. Starting from these secondary building units, it is assumed that these regularly connect to ladders or linear chains which then themselves aggregate to produce the observed 1D-SNF.

3.8.2. Surface-curvature-based mechanism

Gao and McCarthy suggested a mechanism for 1D-SNF synthesised by evaporation of an azeotrope of TMCS and TCS which is based on surface-curvature effects [9]. XPS investigations revealed that TMCS and TCS react in a ratio of ~1 / 10. While TCS can polymerise in all dimensions after hydrolysis, TMCS will terminate the spatial growth because of only one reactive hydroxyl group. In addition, because of the superhydrophobicity of surfaces coated with these 1D-SNF, the researchers concluded that the hydrophobic methyl groups of the trimethylsilane cover 1D-SNF surface. The sterically demanding Me_3Si-groups shield subjacent and unreacted hydroxyl groups close to the surface of the fibre. The efficiency of this shielding effect is considered to depend on the local surface curvature. The higher the surface curvature, the lower is the shielding effect. Thus, the highest condensation

rate is expected to occur at the highly curved tips and not at the less curved sidewalls of the fibres. This discrimination finally leads to the growth of one-dimensional structures.

3.8.3. Diffusion-based mechanism

From the systematic studies of the growth conditions (see chapter 3.5) Rollings and Veinot concluded that (1) hydroxyl groups on the surface are necessary for fabricating a coating, (2) the amount of water adsorbed on the surface needs to be in a certain range and (3) the reaction is diffusion limited with respect to the transport of the silane to the surface. From these findings, the following mechanism is suggested [16]. The first incoming silane molecules are hydrolysed in the gas phase or in the water layer on the surface. These silanols anchor to the hydroxyl groups of the substrate surface and act as nucleation sites for further growth. A high density of hydroxyl groups is considered to reduce surface diffusion of the silanol species which in turn leads to small polymeric islands by further condensation at the initial nucleation sites. These islands then start to extend into the gas phase. As a consequence, the protruding tips of the polymeric islands are more exposed to the gas phase than the subjacent substrate surface. Thus, diffusion of silane molecules to the tips of the islands is more efficient than diffusion to the substrate in between. Preferred deposition and the reaction of silane at the tips of the islands occur, which leads to one-dimensional growth and finally the formation of fibres.

3.8.4. Gold particles as templates

A mechanism using gold particles as templates is presented for the formation of 1D-SNF in a solution [69]. In the presence of water, the surface of gold nanoparticles serves as a catalyst to hydrolyse the Si–H bonds of the precursor ODS forming octadecylsilanol species. The silanols then condense yielding the polysiloxane. Here the gold particle functions as a templating agent ‘restricting the polymer structures to mostly one dimension’ [69]. Therefore, the diameter of the 1D-SNF can be expected to correlate with the size of the gold particles.

The final 1D-SNF still contain the gold particle at the tip. Without water or gold particles present, the formation of 1D-SNF is not observed.

3.8.5. Discussion of suggested mechanisms

The ratio of $MeSiO_{1.5}$ to MeSiO(OH) found to be 1 / 3 by Chen et al. [11] is remarkable. The existence of a considerable amount of unreacted hydroxyl groups in the 1D-SNF matches the observations of Zimmermann et al. and Nouri et al., who reported improved superhydrophobicity [18, 63] and chemical stability [18] after thermal annealing. Both effects can be well explained by the condensation of hitherto unreacted hydroxyl groups in the 1D-SNF upon heating. The further conclusions i) the two building blocks $MeSiO_{1.5}$ and MeSiO(OH) regularly condense to secondary building blocks because of their ratio 1 / 3 and ii) these secondary building blocks in turn connect in a regular manner are questionable [11]. A priori, it is not clear that 'under equilibrium conditions, each CH3SiO1.5 is connected with three CH3SiO1.0(OH)1.0 to form a secondary building unit …' [11]. Even if this was the case the assumption of equilibrium conditions is invalid during the growth of 1D-SNF.

The proposed aggregation into ladder or chain-like structures should be detectable by diffraction experiments. In fact, other researchers concluded from such experiments that the 1D-SNF are amorphous [8, 69].

Discrimination of reactive surface sites by the surface curvature was proposed by Gao and McCarthy [9]. However, this mechanism works only for the specific mixture of a multifunctional and a monofunctional silane. The formation of the vast majority of reported 1D-SNF grown from only one silane of the type $RSiX_3$ can not be explained by this mechanism.

The extensive experimental observations by Rollings and Veinot, especially the necessity of hydroxyl groups at the surface, the appropriate amount of adsorbed water and the diffusion-limited growth, are well reflected in the mechanism proposed by the same researchers. Especially for the initial growth of the 1D-SNF, this mechanism seems plausible. However,

the longer the 1D-SNF grow, the more they entangle and bend. In this state, the position and orientation of the tips of the 1D-SNF are much more random than those at the beginning. Thus, the preferential deposition of precursors no longer would solely occur at the tips but at those parts of the 1D-SNF which are most exposed to the atmosphere. It is difficult to imagine that the formation of curved and entangled 1D-SNF with lengths up to micrometres and practically constant diameter merely proceeds via the proposed diffusion-based mechanism. To summarise, in our opinion, not all necessary aspects to explain the formation of 1D-SNF on surfaces have been explored satisfactorily.

4. Chemical modification

4.1.1. Oxidation

Annealing of 1D-SNF with a vinyl group as an organic residue at 1000 °C for 1 h resulted in a very hydrophilic surface [10]. Electron microscopic investigations showed that the filamentous morphology did not change because of the heat treatment. Data obtained by XPS suggested that all organic groups were oxidised. The annealed surfaces were superhydrophilic. A water contact angle below 5° was reported.

Chen et al. reported similar results [11]. According to thermal gravimetry and differential thermal analysis, condensation of hydroxyl groups occurred below 480 °C. Above this temperature, the oxidation of methyl groups began. After performing calcination in air at 500 °C for 1 h the superhydrophobic properties gave way to superhydrophilicity. However, here the filamentous topography of the coating was destroyed. The conversion to superhydrophilic behaviour was also obtained by irradiation with UV light for 12 h.

The oxidation of the 1D-SNF can be performed within minutes by treatment in oxygen plasma [35, 41, 42], water plasma [29] or oxygen / hydrogen plasma [60–62]. The oxidation of the organic residues of polysiloxanes leads to a silica-like surface containing hydroxyl groups [79]. Therefore, the oxidised surfaces become superhydrophilic, and contact angles

with water range close to 0°. EM revealed that the specific filamentous topography of the 1D-SNF coating remained unaltered by plasma treatment [35].

4.1.2. Reactions of oxidised 1D-SNF

The hydroxyl groups produced on the surface of the 1D-SNF by oxidation are well suited for further chemical modification by condensation with silanes. Functionalisation with OTS [35], PFOTS [35, 60–62], PFDTS [24], aminopropyl triethoxysilane [41], 2-(carbomethoxy)ethyl trichlorosilane [41], 3-(2-bromoisobutyryl)propyl dimethylchlorosilane and subsequently polymer brushes [42], 3-(2-bromoisobutyryl)propyl triethoxysilane and subsequently a poly(methacrylic acid)-based polymer [29] and titania nanoparticles [43] is reported. The potential applications based on these modifications are reviewed in chapter 6.

4.1.3. Plasma fluorination

Direct fluorination without prior oxidation of the 1D-SNF was used by Artus et al. in order to achieve superoleophobicity (see chapter 6.2) [34]. The applied pulsed plasma polymerisation process deposits a perfluoroacrylate coating with a very low surface energy onto the 1D-SNF [80].

5. Properties of 1D-SNF

5.1. Single 1D-SNF

5.1.1. Morphology

Obviously, the most characteristic property common to all 1D-SNF is the one-dimensional morphology with an extreme aspect ratio. Mostly, diameters around 40 nm are found by EM and scanning force microscopy [6–12, 16, 28, 29, 43, 55, 56, 69]. The observed values range from 10 nm to 100 nm. Artus et al. observed 1D-SNF around 150 nm in diameter in addition to thin 1D-SNF on the same sample [8]. The diameters of nanotubes were reported to be even larger [56]. Simultaneously, maximum lengths of 1D-SNF grown onto surfaces are reported to range from several hundred nanometres to several micrometres. For 1D-SNF with

embedded gold particles grown in the solution, lengths approaching 1 mm were observed. These dimensions imply a remarkable maximum aspect ratio on the order of 10^4.

5.1.1.1. Massive 1D-SNF

All published EM images show 1D-SNF with a remarkably uniform diameter along the entire length of the filament. Small variations around some mean diameter are reported by Khoo and Tseng [12]. In this case, the 1D-SNF are not smooth like a wire, but resemble a chain-like or string-of-pearls-like periodic assembly of particles.

Specific cross sections of massive 1D-SNF are not reported. From the published EM images, the 1D-SNF seem to have round cross sections throughout indicating an amorphous material. Results from TEM did not indicate crystalline nature within the 1D-SNF [8, 69].

With increasing length, the 1D-SNF were found to be contorted increasingly. 1D-SNF curled into spirals were reported by Prasad et al. and Zimmermann (figure 5) [38, 69].

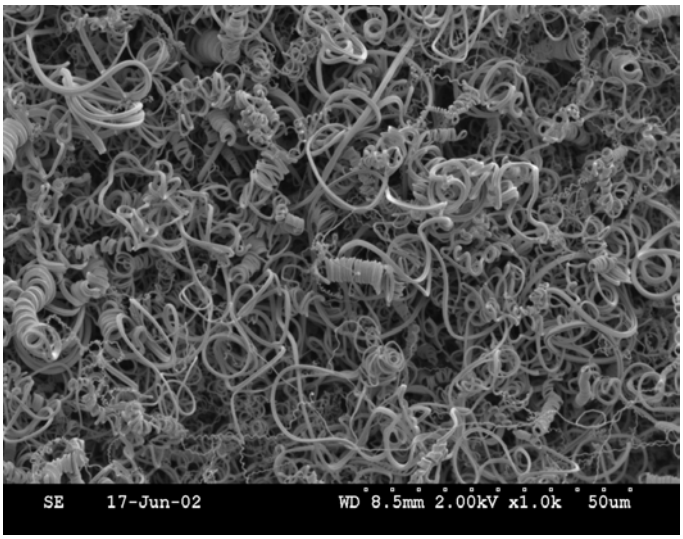

Figure 5. EM image of curled 1D-SNF. Adapted from [69] with permission. Copyright 2003, American Chemical Society.

As a consequence of contortion, the entanglement among 1D-SNF is increased. Thus, with longer 1D-SNF, a layer of 1D-SNF is often described as a quasi-three-dimensional network.

Currently, there is little knowledge about the nature of the cross linking between 1D-SNF in these networks. It is difficult to distinguish between branching, adhesion and chemical bonding between 1D-SNF, e.g. by inter-filamentous condensation of residual hydroxyl groups, by considering EM images alone. Branching, i.e. splitting a filament into two branches during the growth of the 1D-SNF is reported only once [12].

Force–displacement curves measured by a scanning force microscope indicate adhesion of 1D-SNF at the tip of the cantilever and disentanglement on retraction of the tip, demonstrating the flexibility of the 1D-SNF [8].

5.1.1.2. Tubular 1D-SNF

Stojanovic et al. reported the synthesis of partially or completely hollow 1D-SNF [56]. Tapered 1D-SNF with diameters from 200 nm to 700 nm at the base and 60 nm to 200 nm at the tip were obtained in a gas phase reaction. The maximum length equalled 12 µm. While the tips enclosed a cavity, the bulk was found to be massive. By varying the coating conditions, microtubes up to 4 µm in length with diameters approaching the micrometre range could be obtained. 1D-SNF being hollow over the entire length could be synthesised in solution [56]. A maximum length of 5 µm and external diameters in the range 80 nm to 100 nm were determined. The interior diameter was found to be 10 nm to 20 nm. At the end of the tubes the channels widened.

1D-SNF with embedded gold nanoparticles grown in the solution are claimed to exhibit a tubular structure to some extent [69].

5.1.2. Chemical composition

The chemical composition of the 1D-SNF is examined by XPS [6, 10, 12, 14, 16], FT-IR or ATR-IR [10, 11, 13, 30, 55, 56], energy-dispersive X-ray spectroscopy [10, 13, 30, 55, 56, 69], time-of-flight secondary ion mass spectroscopy [10, 16], Auger electron spectroscopy [16], elemental analysis [69] and thermogravimetric analysis [11]. All methods confirm the

1D-SNF to be composed of polysiloxanes with organic residues corresponding to those of the monomers used.

Stojanovic et al. found traces of the elements calcium, potassium, sodium, aluminium and chlorine at the tip of 1D-SNF. The glass substrate was suspected as source of these ions. When magnesium chloride was introduced into the system prior to the coating magnesium was again detected only at the hollow tip of the 1D-SNF.

A special case is the 1D-SNF grown from a mixture of TMCS and TCS reported by Gao and McCarthy [9]. By XPS, it was shown that the ratio of TCS / TMCS in the product is ~10 / 1. The actual degree of condensation remains unclear in most analyses. However, for 1D-SNF obtained from methyltrialkoxysilanes, a sum formula of $CH_3SiO_{1.12}(OH)_{0.76}$ is reported by Chen et al. [11]. On the basis of kinetic considerations, it is argued that the 1D-SNF consist of the molecular building blocks $CH_3SiO_{1.5}$ and $CH_3SiO(OH)$ in a ratio of 1 / 3. This corresponds to a degree of condensation of 75%.

5.2. Microscopic and macroscopic properties of 1D-SNF-coatings

5.2.1. Thickness

The high density of entangled 1D-SNF gives rise to a coating on the substrate. The thickness of the coating obviously correlates with the length of the 1D-SNF and thus with the coating conditions (chapter 3.5). Coatings described as fibrous mats with thickness exceeding 1 µm were reported by Rollings and Veinot [16]. Khoo and Tseng observed varying layer thicknesses depending on the growth conditions up to 320 nm [12]. Artus et al. found a layer thickness of at least 60 nm by scanning force microscopy and 141 nm by ellipsometry [8]. Zhang and Seeger observed coatings from 600 nm to 7 µm in thickness (figure 6) [24].

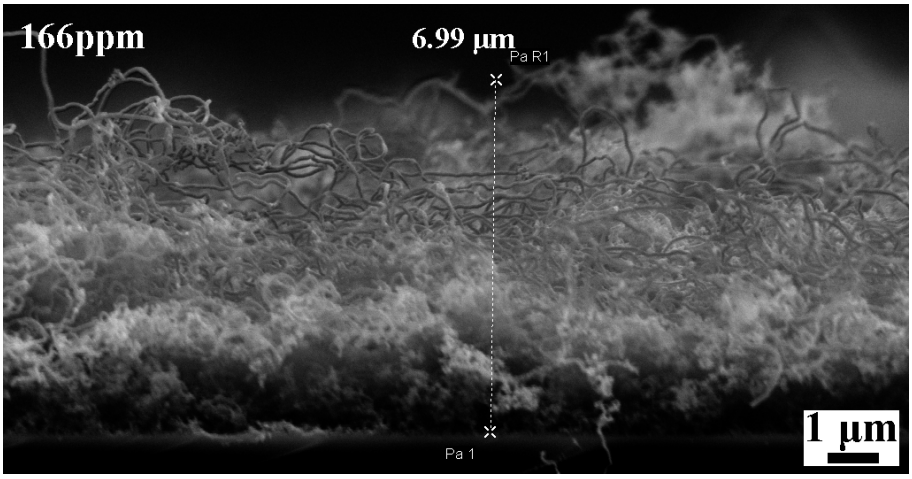

Figure 6. EM image of a 1D-SNF-coating with 7 µm in thickness. Adapted from [24] with permission. Copyright 2011, Wiley-VCH.

A quantity related to the thickness of the layer is the mass of deposited polysiloxane. A mass fraction of the polysiloxane of 1.86% was determined by Shateri-Khalilabad and Yazdanshenas [55]. The substrate was cotton which was made conductive with graphene prior to the coating of 1D-SNF. A similar gain in mass of 2% was found by Shirgholami et al. on cotton [30].

5.2.2. Optical properties

The thickness of the coating determines the optical appearance of the coated substrate. Thicker coatings appear opaque or hazy because of light scattering. Fluorination of the coating by PFDTS additionally lowers the transmission by approximately 6% [24]. Samples with thin coatings are nearly indistinguishable from uncoated samples by eye. On transparent samples, the coatings can even have an anti-reflective effect [8]. On a glass slide coated on both sides, transmittances higher than 95% in the visible range were reported (figure 7) [39]. Comparable optical properties were reported by other groups [28, 57, 64]. A refractive index of 1.12 of the coating was measured by ellipsometry [8].

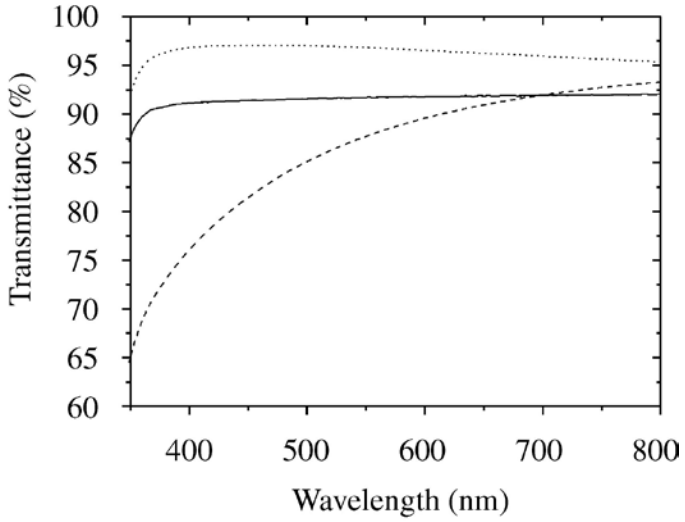

Figure 7. Transmission spectra of glass slides coated on both sides. A thin coating (· · · · · ·) reduces the reflectivity whereas a thick coating (- - - -) reduces transmission of light compared to an uncoated glass slide (——). Adapted from [39] with permission. Copyright 2008, Taylor & Francis.

5.2.3. Water repellency

Probably, the most noticeable property of 1D-SNF coatings is their water repellency. Water does not wet any coated surface and forms nearly spherical drops, which roll off at very low inclination angles. Dynamic and static contact angles around 170° and sliding angles of a few degrees depending on the type of the substrate and coating conditions were reported by several researchers (see chapter 3.5) [8, 9, 12, 15, 24, 56, 57]. Post-treatment of the 1D-SNF, such as thermal annealing or exposure to trimethylsilyliodide, enhances the water-repellent properties [7, 8, 18, 19, 63]. Hence, 1D-SNF coatings certainly belong to the most water-repellent surfaces known. This is especially remarkable since the 1D-SNF coating is fluorine free. Very often fluorination of surfaces is needed to achieve superhydrophobicity. The reasons for the superhydrophobic behaviour are the hydrophobic nature of polysiloxanes and the specific topography of the coating implying very high surface roughness. As a consequence, a water drop resides only on the highest asperities of the surface and does not penetrate into the voids underneath. The high contact angles are described by the Cassie–

Baxter equation: $\cos \theta_a = f_1 \cos \theta - f_2$ [81], where θ_a is the apparent contact angle on a rough surface, θ is the contact angle on a flat surface of the same material, and f_1 and f_2 are the fractions of solid–liquid and liquid–air interfaces underneath the drop, respectively. The main reasons for the high apparent contact angles are the low solid–liquid fraction and the correspondingly high liquid-air fraction. These fractions were determined by Zhang and Seeger for 1D-SNF coatings on a substrate with two-tier roughness consisting of silica beads on glass [57]. For a contact angle of 179.8° and sliding angle of 1.3° f_1 and f_2 were 4.8% and 95.2%, respectively. Similar values were found by Shirgholami et al. for 1D-SNF coatings on a cellulose fabric [30]. On the most water-repellent sample with a contact angle of 166.7° f_1 and f_2 were 4% and 96%, respectively. A more general discussion on wetting of superhydrophobic surfaces is beyond the scope of this review. We refer the reader to read recently published reviews on this topic [76, 82].

A property of 1D-SNF coatings is the flexibility of the 1D-SNF [8]. In the wetted state, it can be anticipated that the meniscus forces deform or reorient single 1D-SNF underneath the drop and at the contact line. The impact on the contact angle, sliding angle or hysteresis is unknown. In addition, there exists no theory describing this situation since standard wetting theories assume fixed substrates. It is surmised that the surface flexibility on the length scale of the 1D-SNF might have a similar enhancing effect on wetting [8], as it is described for surfaces exposing liquid-like and movable alkyl chains on the molecular scale [83, 84].

Rollings et al. reported static contact angles of 137° [10] and advancing and receding contact angles of 131° and 127°, respectively [16], for their 1D-SNF synthesised from vinylsilanes. These are lower contact angles compared to those reported by others probably because of the presence of a double bond in the organic residue. For 1D-SNF composed of a copolymer synthesised from a mixture of VTS and TFPTCS, an advancing contact angle of 161° was found [16]. Gao and McCarthy observed advancing and receding angles of 176° and above by also using the sessile drop method for measuring contact angles [9]. However, this standard

method was found to be not sufficiently precise for such high contact angles. Therefore, they applied a newly developed contact/compression/release method, where the drop is contacted from above (figure 8) [17]. Applying this method, advancing and receding contact angles of 180° were measured, and zero adhesion energy was noted [7].

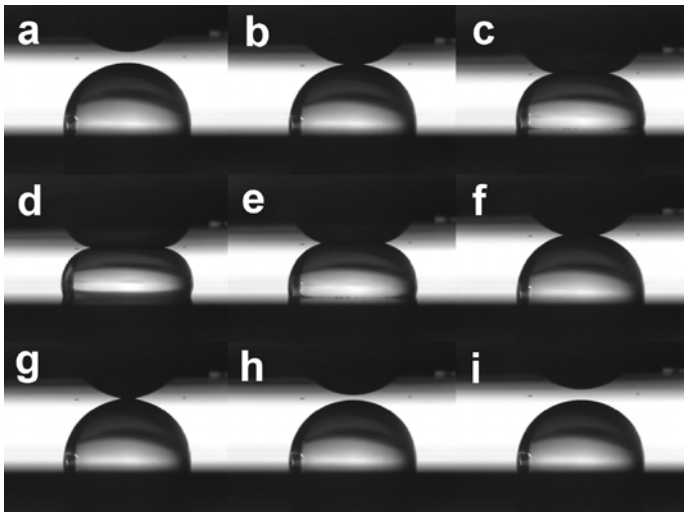

Figure 8. Selected frames from a video of a 1D-SNF coating contacting, compressing and being released from a sessile water droplet demonstrating the contact angle of 180°. Adapted from [9] with permission. Copyright 2008, American Chemical Society.

Advancing and receding contact angles of 180° were confirmed by Chen et al. also employing the contact/compression/release method [3]. Extremely low sliding angles below 1° were also found on samples coated with nanotubes [56].

For the characterisation of hydrophobicity of rough and non-reflecting samples—such as textiles—contact and sliding angles were found to be insufficient measures [14]. For this type of sample, the 'shedding angle' was introduced by Zimmermann et al. [20]. This method determines the minimum inclination angle at which an impacting droplet does not penetrate the surface but rolls off without leaving a trace. Shedding angles below 5° were reported for

[3] The question on how to determine exact contact angles close to 180° in practice is not answered finally. The problem is the flattening of the drops because of gravity. For drop volumes in the microlitre range, as they are mostly applied in the studies cited here, it is known that the standard sessile drop method tends to underestimate contact angles on superhydrophobic surfaces [85, 86].

coated polyester fabrics [14, 40]. The classical sliding angle for a 10 µL drop on the same surface would be ~15°. A water jet easily bounces off these surfaces. For fabrics made of other materials, the shedding angles ranged from 5° to 55° [14, 55]. The actual type of movement of a water drop on an inclined 1D-SNF coating, rolling, sliding or combinations thereof [87], is unknown.

Beyond contact angles and sliding angles or hysteresis for water (the standard test liquid), similar data for many other liquids such as organic solvents, diiodomethane or ionic liquids have been reported. Contact angles above 150° were achieved for thiodiethylene glycol (γ = 53.5 mNm^{-1}) and liquids with higher surface tension. Table 3 summarises contact and sliding angles reported in the literature to date.

In contrast to the superhydrophobicity of 1D-SNF coatings, they are also superoleophilic without further treatment. Oily liquids such as hexadecane or crude oil easily wet and penetrate the coating (compare chapter 6.2) [35, 40].

Liquid	Surface tension / mN/m	Contact angle / °	Sliding angle (s) or advancing and receding contact angles (ar) / °
Hexadecane [35]	27	~2	s > 90
Cyclopentanol [6]	32.7	7 ± 1	-
Ethyl cinnamate [6]	37.17	22 ± 4	-
Diethylene glycol [6]	44.6	112 ± 2	-
Ethylene glycol [6]	48	148 ± 5	-
1-Ethyl-3-methylimidazolium tetrafluoroborate[a] [88]	49.2	122, 130	ar 113, 113
1-Ethyl-3-methylimidazolium ethylsulfate[a] [88]	49.4	126, 126	ar 117, 116
Ethylene glycol ferrofluid [60]	50.28	-	ar 169, < 4

Diiodomethane [24, 35]	50.8	90.9 [24], 115 ± 4 [35]	s > 90 [24, 35]
Thiodiethylene glycol [6]	53.5	156 ± 5	-
Glycerol anhydrous [6]	62.7	162 ± 5	-
1,3-Dimethylimidazolium methylsulfate[a] [88]	64.2	175, 170	ar 165, 160
Dimethyl-di(2-hydroxyethyl)-ammonium methylsulfate[a] [88]	66.4	174, 118	ar 166, 110

Table 3. Contact angles and sliding angles for different liquids as measured on fluorine-free 1D-SNF coatings. a) Ionic liquid. The two values for the contact angle correspond to measurements on 1D-SNF synthesized from pure TCMS or from a mixture of TMCS/TCS.

5.2.4. Durability

5.2.4.1. Short-term durability

1D-SNF coatings were found to be insensitive to UV irradiation, water vapour under enhanced pressure and liquid nitrogen [6, 8, 19].

As for all surfaces with roughness on the nanoscale mechanical wear is a major problem also for superhydrophobic surfaces (figure 9) [89]. Abrasion tests in a friction analyser confirm the low mechanical stability of the coating on flat substrates [14]. Nevertheless, the water-repellent properties suffer much less from mechanical wear when coating a macroscopically rough textile with 1D-SNF. An abrasion test identical to the one reported for glass showed severe abrasions at the most exposed fibres of the textile. However, the coating for fibres buried deeper in the three-dimensional structure of the textile the coating remained intact. Thus, the overall superhydrophobicity of the sample was reported to be maintained (figure 9).

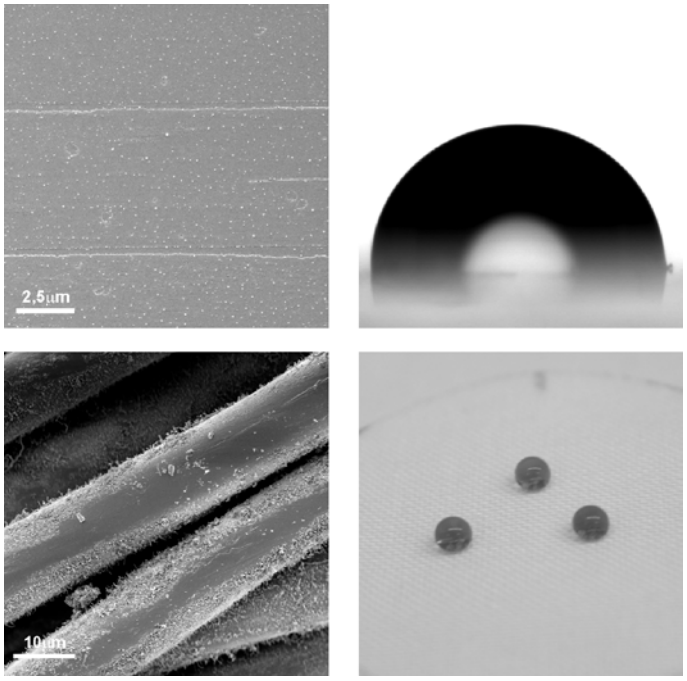

Figure 9. SEM images of coated samples after the abrasion test and photographs of drops of water showing the wetting properties of the abraded samples. Top: glass surface. Bottom: Polyester fabric. Adapted from [14] with permission. Copyright 2008, Wiley-VCH.

Contrary to this, machine washing of a 1D-SNF-coated cotton sample led to mechanical and chemical deterioration of the 1D-SNF. Although impinging drops of water were still repelled by the washed sample, a sessile drop of water would be absorbed by the fabric after a few ten seconds [14]. Similar findings were reported by Shirgholami et al. [30] on a coated cellulose fabric after five cycles of washing. Contact angles decreased by approximately 8°. The deterioration of sliding angles was considerably higher, especially for drops of low volume. Zhang and Seeger subjected their fluorinated and superoleophobic coatings to different environmental conditions [24]. As can be expected from the superior chemical stability of the 1D-SNF due to fluorination, no obvious change in contact or sliding angles was noticed subsequent to heating in air or irradiation with UV light, exposure to outdoor conditions for two weeks, exposure to ozone, immersion in a 1 M NaOH solution or sulphuric acid for 1 h. The mechanical stability did not improve because of fluorination.

5.2.4.2. Long-term durability

Zimmermann et al. reported studies on the long-term durability of the 1D-SNF coatings under different chemical conditions [18]. Glass cover slips coated with 1D-SNF were constantly immersed in solvents or solutions for a total period of 182 days. In ethanol, acetone and toluene only small deviations of contact and sliding angles were observed, depending on the polarity of the solvent. The morphology of the 1D-SNF remained unchanged. In alkaline solutions at high pH values, the coating was reported to decompose within one day (figure 10). For all other pH values, the contact angles were stable for at least 10 days. Sliding angles were found to be more sensitive and slowly increased from the beginning of the immersion despite for pH values 6.7 and 3. For at least 10 days, the sliding angles were below 70° for all pH values below 11. In addition, the filamentous morphology was still observed by EM after 6 months of immersion at pH 6.7 or 3. For pH values above 11, severe damage because of etching was observed.

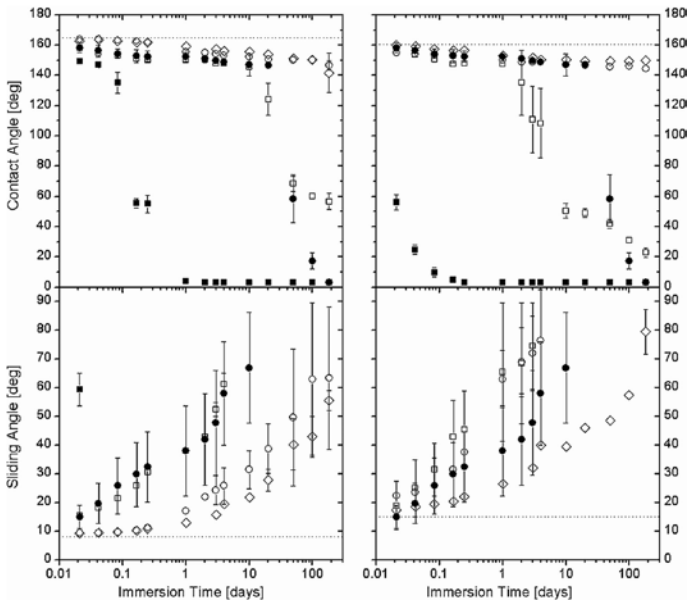

Figure 10. Contact and sliding angles of annealed (left) and non-annealed (right) samples as a function of immersion time in aqueous solutions (■ pH 13, □ pH 11, ☐pH 6.7, ○ pH 3, ● pH 0). The dotted lines indicate initial values. Adapted from [18] with permission. Copyright 2007, Elsevier.

The stability of the coating is attributed to the air cushion between the solution and 1D-SNF (see chapter 5.2.6). It is argued that the area of the solid–liquid interface where etching can occur is reduced greatly. Thus, the deterioration of the complete layer is retarded. This air layer is no longer observed when the coating is immersed in surfactant solutions. However, the stability was found to be better compared to solutions with the same pH value but without surfactant. The reason is assumed to be protection of the 1D-SNF by an adsorption layer of surfactant molecules. In general, annealed samples are reported to show much better chemical resistance than non-annealed samples.

In a second study, environmental effects were investigated with respect to potential outdoor applications [19]. During one year of outdoor exposure, the contact and sliding angles of a coated glass slide changed from initially 155° to 148° and 21° to 69°, respectively. The filamentous morphology of the coating was shown to be still present after one year, although heavily clogged with contaminants. Nevertheless, images captured by a webcam positioned behind the coated glass demonstrated a much better water repellence compared to an uncoated sample. In addition, the transmittance of coated slides was reported to be 5% better than that of uncoated slides after one year of outdoor exposure. An ‘acid dew and fog’ test was also conducted. During this test, the sample was continuously exposed to acids, UV irradiation, artificial rain and drying phases. Only slight deterioration in the wetting properties was observed after three weeks of exposure, after which more severe degradation occurred.

5.2.5. Self-cleaning

The self-cleaning effect of superhydrophobic surfaces is well known [90, 91]. In spite of this fact, systematic investigations on the self-cleaning effect of 1D-SNF coated surfaces have not been published. The self-cleaning effect of 1D-SNF on a polyester fabric is briefly mentioned by Artus and Seeger [21]. Wong et al. reported the removal of silica powder (placed as a contaminant onto a 1D-SNF-coated glass slide) by the action of a water drop [28, 64].

5.2.6. Plastron in water and organic liquids

The heterogeneous Cassie–Baxter type of wetting implies that water wets only the highest asperities of a superhydrophobic surface. Thus, a 'dry' layer composed of air and 1D-SNF was formed in between the substrate and water. Because of its low refractive index, it causes total reflection of light. Therefore, a 1D-SNF-coated sample immersed in water seems to be covered by a silvery and shiny layer, a so-called plastron [33]. When the plastron is thicker compared to the wavelengths of visible light, the total reflectance is more pronounced. This is in accordance with the reported thickness values for the 1D-SNF coatings ranging up to 7 µm. This plastron was observed on glass, polyester and silicon coated with 1D-SNF (figure 11). Furthermore, it was found to be stable over a duration of weeks [14, 39, 40, 59].

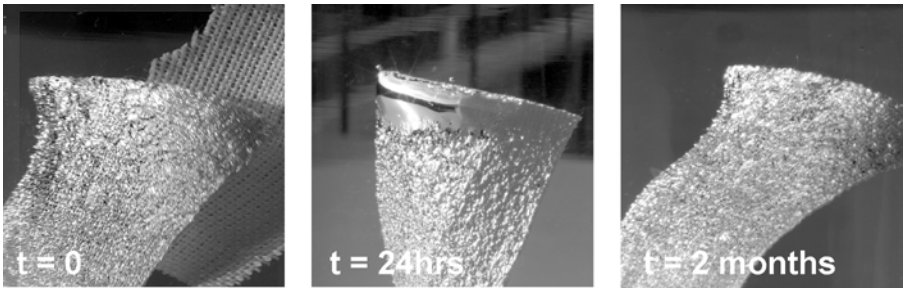

Figure 11. Plastrons observed on a piece of polyester fabric coated with 1D-SNF and immersed in water. The left image shows a piece of uncoated fabric without a plastron in the background. Adapted from [14] with permission. Copyright 2008, Wiley-VCH.

The existence of a plastron in solvents with low surface tension has also been demonstrated. Zhang and Seeger reported a plastron in toluene for glass samples which were rendered superoleophobic by plasma oxidation of the 1D-SNF coating and subsequent reaction with PFDTS (see chapter 6.2) [24]. Artus et al. showed the existence of a plastron in hexadecane and in heptane on a superoleophobic polyester fabric [34].

6. Applications

6.1. Water repellency

A 1D-SNF coating was used by Asanuma et al. to investigate the structure of water at the interface of a superhydrophobic surface with bulk water by sum frequency generation spectroscopy [92]. The virtues of the 1D-SNF coating for these experiments are twofold: (1) the coating could be easily applied to a quartz prism, which was used to contact the water, and (2) the coating is transparent, a major prerequisite for the investigation by optical means. The results indicate 'a stable water/air/solid three-phase interface even though the sample is completely immersed in water'. The interface of the water and the superhydrophobic substrate resembled an air/water interface. This implies that water comes into contact only with the highest asperities of the solid surface.

1D-SNF coatings were used by Korhonen et al. for investigations of the reliability of contact angle measurements [61]. By varying the coating protocols, surfaces with varying wettability and varying contact angle hysteresis were obtained. These surfaces were employed for measurements of the advancing and receding contact angles. The results were used to validate a theoretical model to estimate the necessary drop volumes for the reliable measurement of advancing and receding contact angles.

Similar variations of 1D-SNF coatings were also used by Timonen et al. [60] for experiments with magnetic fluids on superhydrophobic surfaces. Magnetic nanoparticles were dispersed in water or ethylene glycol. Thus, the droplets could be oscillated, driven or manipulated by magnetic fields. The different wetting properties of 1D-SNF coatings, among other surfaces, resulted in different friction coefficients for the movement of the droplets. This effect was exploited for the investigations of the static and dynamic self-assembly of magnetic droplets on superhydrophobic surfaces. The same surfaces were also used for the investigation of the dissipation of energy of magnetically manipulated droplets on superhydrophobic surfaces [62].

Wong and Yu suggested to use the coating process and the determination of the water repellency of 1D-SNF coatings as demonstration for undergraduate teaching [64].

6.2. Oil repellency

A reaction of an oxidised 1D-SNF coating with OTS in toluene restores the pristine superhydrophobicity with water contact angles above 160° [35]. Using PFOTS instead of OTS led to oleophobic surfaces. Zimmermann et al. reported contact angles of 140° and 165° with hexadecane and diiodomethane, respectively, on 1D-SNF-coated glass substrates [35]. By reacting 1D-SNF-coated glass substrates with PFDTS in toluene subsequent to oxidation, Zhang and Seeger achieved superoleophobicity (figure 12) [24].

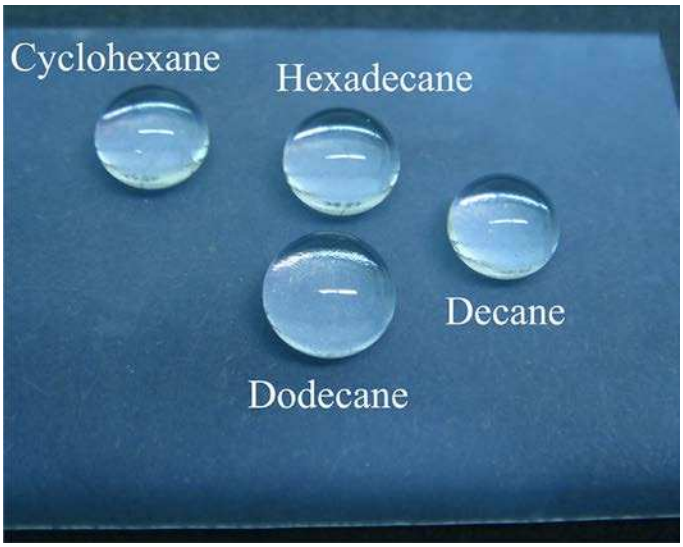

Figure 12. Droplets of various non-polar liquids on a fluorinated 1D-SNF-coated glass slide. Adapted from [24] with permission. Copyright 2011, Wiley-VCH.

For several organic liquids with surface tensions between 32 and 23.8 mNm^{-1}, such as mineral oil, toluene or *n*-decane, contact angles above 162° and sliding angles below 6° were reported. With water, contact angles above 170° and sliding angles below 10° were published. Superoleophobicity on a polyester fabric was reported by Artus et al. [34]. Plasma fluorinated 1D-SNF-coated polyester fabrics obtained the highest possible oil repellency grade of eight.

This means that a static drop of heptane is stable for at least 30 s on the substrate and does not penetrate [93]. Furthermore, the dynamic repellency of impacting drops of liquid alkanes was tested by the shedding angle method [20]. Shedding angles from 20° to 25° for *n*-hexadecane and *n*-dodecane, 30° for *n*-decane and 48° for *n*-octane were reported. By comparison with reference samples, it was demonstrated that a dense and thick 1D-SNF coating was necessary for improving of the oil repellency, whereas a low and incomplete coverage with only short 1D-SNF was detrimental.

6.3. Separation of oil and water

The superhydrophobic and superoleophilic properties of the coating were used by Zhang and Seeger for the separation of oil and water [40]. While water is repelled by a 1D-SNF-coated piece of polyester textile, oily substances easily penetrate it. A mixture of octane and an aqueous solution poured onto the coated fabric was separated completely. Water resided on top of the fabric while octane was present underneath it. This separation process could be repeated several times without a loss in superhydrophobicity or separation efficiency. In a second experiment, a bag made from a coated textile and filled with an oil absorbing material was immersed in a mixture of crude oil and water. Only crude oil was selectively absorbed and not water.

6.4. Switchable wettability

The transparency and the possibility of chemical modification of 1D-SNF coatings was utilised by Hua et al. to produce transparent surfaces which can be reversibly switched from superhydrophobic to superhydrophilic by counter ion exchange [29]. A 1D-SNF coating was activated in water plasma and reacted with 3-(2-bromoisobutyryl)propyl triethoxysilane. The bromoisobutyryl moiety was used as surface-bound initiator for the subsequent co-polymerisation of 2-(methacryloyloxy)ethyltrimethylammonium chloride and ethyl-2-bromoisobutyrate in the presence of trifluoroethanol. The reaction finally yielded a poly[2-(methacryloyloxy)ethyltrimethylammonium chloride-*co*-trifluoroethyl methacrylate]-tethered

surface. The water repellency was switchable by counterion exchange in methanolic solutions of either sodium chloride or sodium perfluorooctanoate. With chloride, a superhydrophilic surface with a water contact angles of 3° was obtained. A contact angle of 164°, and thus superhydrophobicity, resulted from perfluorooctanoate as counterion. The wettability could be switched several times reversibly.

6.5. Patterning of wetting properties

The polymer-tethered surface presented by Hua et al. [29] (see chapter 6.4) could easily be transformed to a surface with superhydrophilic and superhydrophobic domains by patterning the distribution of chloride and perfluorooctanoate counterions. Since the superhydrophilic surface had anti-fogging properties but not the superhydrophobic one the pattern was visible in moist air or steam. The superhydrophilic parts were transparent, the superhydrophobic parts opaque. This property was used to selectively obscure information and to write and erase information by corresponding patterning.

Oxidation and subsequent modification with silanes was used in combination with partial masking of the substrates to produce samples with patterned wetting properties [35]. An initially superhydrophobic sample coated with 1D-SNF was partially masked and then subjected to oxygen plasma. Subsequent reactions with PFOTS only rendered the oxidised parts of the sample oleophobic (contact angle of 140° with hexadecane and 165° with diiodomethane). By another oxidising step, now masking the oleophobic part and parts of the remaining original 1D-SNF coating, further areas of the original coating could be oxidised, rendering them superhydrophilic and superoleophilic. The resulting sample showed three different wetting regions: superhydrophobic/superoleophilic, superhydrophilic/superoleophilic and superhydrophobic/oleophobic. As shown by wetting of solutions of a fluorescent dye, superhydrophilic canals with a width below 1 mm could be produced on a superhydrophobic background.

Stojanovic et al. presented a method for fabricating a wettability contrasted superhydrophobic/hydrophilic material to the micrometre scale [36]. This was achieved by ablating the 1D-SNF coating from a glass substrate using a UV laser. The ablated areas were hydrophilic with a contact angle of 57°. Hydrophilic patches from 1 µm to millimetres in size and of arbitrary shape, e.g. lines, circles or squares, could be produced this way. Staining with an aqueous solution of a fluorescent dye revealed that only the hydrophilic areas were wetted but not the superhydrophobic background. Round hydrophilic patches were used to fix water droplets at this position even when the sample was turned upside down. Applying the laser ablation method to oleophobic samples resulted in a wettability contrast of oleophobic/hydrophilic. This enabled the fixation of an aqueous drop completely surrounded by hexadecane on a substrate (figure 13).

Figure 13. Coloured water droplets in hexadecane 'microvessels'. Adapted from [36] with permission. Copyright 2010, Springer.

6.6. Wettability gradients

Patterning of a 1D-SNF coating was used by Khoo and Tseng in order to produce wettability gradients [37]. Superhydrophilic wedge-shaped areas surrounded by a superhydrophobic background were produced by exposure of the 1D-SNF coating to oxygen plasma using a

photoresist masking technique. The length of the wedge was 12 mm. A 2 µL droplet of water placed on the apex of the superhydrophilic wedge moved along the wetting gradient towards the wide end of the wedge. With an apex angle of 8° a maximum speed of 455 mms^{-1} was reported. At an inclination angle of 90° of the substrate, ascension of the droplet was observed.

The hydrolysis of the 1D-SNF in alkaline solutions was used by Zimmermann et al. to create wettability gradients [38, 39]. By completely immersing a coated glass sample in a sodium hydroxide solution completely and slowly retracting it, slowly contact angles between ~0° and 160° were obtained depending on the immersion time. The achieved gradients were about $16°cm^{-1}$.

6.7. Writing and erasing of information in a plastron

A plastron stabilised by a 1D-SNF coating was used by Verho et al. for writing, erasing, rewriting or storing information [59]. The sample was a silicon wafer patterned with flat microposts of several microns in size and coated with 1D-SNF. On such a sample with two-tier roughness, two Cassie-type wetting states are shown to occur [76, 81]. At low pressure, the water resides only on top of the microposts. The voids between the posts are filled with gas resulting in a plastron layer with a thickness of several microns at these positions. Higher pressure forces the water into the space between the microposts. The thickness of the remaining plastron (on the order of several 100 nm) corresponds to the thickness of the 1D-SNF coating. Reversible and localised transitions between both states were achieved by the introduction or removal of water using a thin needle. Since both wetting states can be easily distinguished by optical means because of the different light scattering properties of the different plastrons, the two wetting states can be considered as bistable logic states to store binary data [59]. A written pattern could be inspected and erased after 30 days of storage.

6.8. Water harvesting

Condensation of water vapour is an important source of water for life-forms living in arid regions without rainfall. Inspired by the water collecting capabilities of the Stenocara beetle [94], hydrophobic and superhydrophobic surfaces have proven to increase the efficiency of water collection by condensation. Chen et al. reported a water harvesting system based on substrates with a superhydrophobic 1D-SNF coating [11]. The water harvesting efficiency is improved by 50% compared to that of a hydrophilic glass as a collection substrate.

6.9. Protein adsorption

Zimmermann et al. investigated the non-specific adsorption of proteins on 1D-SNF-coated glass slides [41]. The possibility to coat glass in a transparent manner with 1D-SNF enabled the use of a surface-sensitive biosensor by supercritical angle fluorescence [95]. On the 1D-SNF coating (made hydrophilic by plasma activation) the adsorption of β-lactoglobulin was more efficiently suppressed than on oxidised PDMS. Furthermore, contrary to PDMS, no adverse hydrophobic recovery of the surface was observed.

Adsorption experiments with charged proteins as a function of pH were reported with 1D-SNF coatings modified by amino (aminopropyl triethoxysilane) and carboxyl groups (2-(carbomethoxy)ethyl trichlorosilane). The selectivity for the adsorption of proteins with a net charge opposite to the surface charge was found to be three times higher for negatively charged proteins and two orders of magnitudes higher for positively charged proteins compared to the adsorption of proteins with the same charge as on the surface. The adsorption and desorption processes are shown to be reversible for five adsorption–elution cycles without change in the adsorption characteristics or deterioration of the 1D-SNF coating. The selectivity of the modified 1D-SNF coating towards the adsorption of different proteins with different net charges is shown by comparing the adsorption of β-lactoglobulin, α-chymotrypsin and lysozyme. On flat aminosilane layers, an enrichment factor of 2 for negatively charged proteins is reported. For the 1D-SNF-coating, this enrichment factor was

found to range between 4 and 7. Positively charged proteins preferentially adsorbed on the negatively charged 1D-SNF coating by a factor of 8–15.

A similar enhancement of protein immobilisation on 1D-SNF-coated substrates compared to flat ones was reported by Iwasaki et al. [42]. They functionalised 1D-SNF on glass with 3-(2-bromoisobutyryl)propyl dimethylchlorosilane and further patterned them with polymeric brushes prepared by the copolymerisation of 2-methacryloylexyethyl phosphorylcholine and glycidyl methacrylate. The specific adsorption of F(ab') fragments of immunoglobulin G was investigated by fluorescence techniques. The capacity for protein immobilisation on a 1D-SNF-coated substrate was found to be higher by a factor of 65 compared to a flat substrate.

6.10. Immobilisation of catalysts

1D-SNF coatings are an ideal candidate for the immobilisation of catalytic particles because of their chemical stability, the possibility of chemical modification, their large surface area and the large variety of potential substrate materials [43]. Meseck et al. used the 1D-SNF coating as a carrier system for photocatalytically active titania nanoparticles (figure 14) [43].

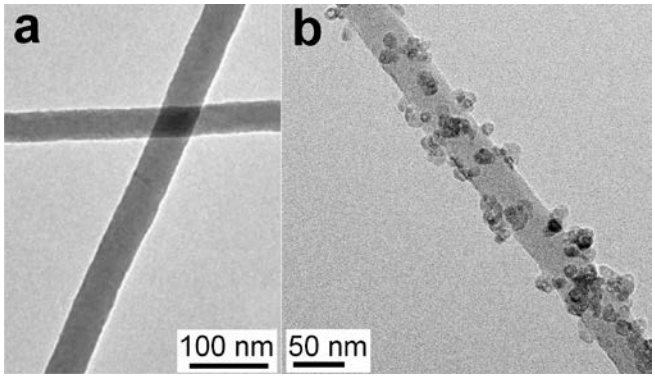

Figure 14. TEM images of 1D-SNF a) before and b) after coating with titania nanoparticles. Adapted from [43] with permission. Copyright 2012, Wiley-VCH.

Titania particles were deposited onto activated 1D-SNF from TiF_4 as a precursor in a water/ethanol mixture at 60 °C. The photocatalytic activity was tested by the degradation of

methylene blue under UV irradiation. At best, 89% of the dye was degraded after 2 h of the reaction. In a control experiment using titania particles on a flat glass substrate, only 32% degradation was measured. The 1D-SNF/titania composite could be reused as a catalytic system at least four times without any loss in performance.

7. Related filamentous structures

One-dimensional hybrid filaments consisting of LPEI and polysilsesquioxane were presented by Yuan et al. [96]. The synthesis required the deposition of nanostructured LPEI filaments onto a substrate in a first step. Subsequently, the LPEI film was used to locally catalyse the hydrolytic polycondensation of a trimethoxysilane which was dispersed in water. The fibrous structure of LPEI also acted as template imparting the final nano-grass-like structure consisting of one-dimensional LPEI@polysilsesquioxane filaments. After treatment with fluorocarbons, the coatings were superhydrophobic and oleophobic. The method also worked for functionalised silanes, e. g. 3-mercaptopropyltrimethoxysilane, which could be functionalised subsequently. Remarkably, the formation of the filaments proceeded in water under nearly neutral conditions. This is probably due to the fact that the catalytic activity of LPEI is similar to that of silicatein, a natural protein catalysing the formation of silica in living systems under physiological conditions [97].

Jin et al. experimented with PFDTS as an educt for the synthesis of 1D-SNF in solvent [98]. The obtained coating consisted of ‘nanofibres and microbumps, which criss cross each other and form a 3D network architecture’. In contrast to the 1D-SNF described in this review, the nanofibres often branch and mostly smoothly interconnect non-fibrous spherical or flat structural units of the three-dimensional network. Although the nanofibres of this study are only a part of a more complex network their similarity to 1D-SNF is remarkable.

The same group reported an effect of the length of the alkyl chain in the trichloroalkylsilane on the surface structure [99]. Mostly non-linear nano-protuberances were obtained. However,

small fractions of fibrous and more linear structures were found when the alkyl residue was a methyl or octadecyl group.

Recently, transparent and elastic aerogels could be synthesised using sol–gel synthesis [100, 101]. Under certain conditions, a specific topography of the aerogel, described as ‘fibrous skeleton’ [101] or ‘continuous fibrous network’, [100] was obtained. The structures observed by EM appear very similar to those of 1D-SNF. Furthermore, the educt for these aerogels is MTMS that implies a very similar composition compared to 1D-SNF. Besides equivalent educts and products, the similarity of both systems extends to the initially acidic reaction conditions, the hydrophobicity and the elasticity of the obtained products [8, 100, 101]. Several researchers reported nanoparticles similar to 1D-SNF in structure, synthesis or superhydrophobic behaviour [102–107]. However, either the existence of one-dimensional particles is not discussed, no or ambiguous analytical data are provided or the true one-dimensional character of the product remains unclear.

8. Future Prospects

8.1. Synthesis

A better and more general understanding of the correlation of coating parameters and properties of the 1D-SNF is desirable. This will help to complete the mechanistic aspects of filament growth and will also allow more targeted syntheses to tailor the properties of the 1D-SNF, especially with respect to their potential applications. This will require mainly two things: (1) on the synthesis side, careful determination of all parameters, e.g. presently the concentration of water in the solvent is often unknown, and a maximum reproducibility of the coating protocols must be achieved. Possibly, this will require clean room conditions. (2) On the product side, a more systematic description of the morphology of filaments, e.g. the distribution of diameters and lengths will be helpful. Furthermore, attention should be paid to alkoxysilanes as educts in order to avoid hydrochloric acid as a detrimental byproduct.

8.2. Mechanism

The formation mechanism of 1D-SNF is one of the most fundamental issues. How and why the 1D-SNF grow is only answered partially (at least as far as the 1D-SNF grown onto surfaces are concerned). Further elucidation of the mechanism of growth will provide the basis for many further steps, e.g. optimising known syntheses, improving the mechanical stability, applying a 1D-SNF coating to hitherto non-coatable substrate materials, tailoring the properties of the 1D-SNF by modifying their morphology, controlling the growth of 1D-SNF or even extending the system to non-silicon-based materials. Understanding the mechanism of growing 1D-SNF will certainly contribute to the rapidly evolving field of nanotechnology of soft matter in general.

8.3. Wetting

Because of the extreme repellency towards water and also organic solvents, the 1D-SNF coating may satisfactorily contribute to the general understanding of wetting. For theoretical calculations of contact angles, a better three-dimensional description of the topography of a 1D-SNF coating beyond the most frequently applied and over-simplified concept of surface roughness is required. Three-dimensional EM techniques may offer an approach to this problem.

The flexibility of the 1D-SNF makes this surface different compared to most other substrates used for wetting experiments. The comparably strong meniscus forces may easily deform or reorient single 1D-SNF underneath the drop or at the contact line. Thus, the wetted surface does not rigidly behave as is assumed in standard wetting theory but responds on the nanoscale to the presence of a liquid. This fact is discussed rarely. The consequences to the situation at the contact line, contact angle, hysteresis or wetting in general are unknown but certainly are worth investigating.

8.4. Applications

The extreme wetting properties of the 1D-SNF coatings have to be mentioned in the first place. With reported contact angles of 180°, the coating belongs to the most water-repellent films known to date. In combination with other advantages such as transparency and chemical inertness of the coating, its applicability on many substrates and its fluorine-free composition are very attractive. Six recent patents and an already conducted scale up of the process also point in this direction [6, 21–23, 25–27]. Applications can be expected with respect to the extreme oil repellency. Nevertheless, without substantial improvement in the mechanical stability, applications will be restricted to single-use devices or environments without mechanical wear. To this effect, applications in microfluidics or water harvesting seem to be promising.

The phenomenon of self-cleaning is highly related to water repellence. Interestingly, systematic experiments on this technically important phenomenon of 1D-SNF-coated surfaces seem to be lacking. In addition, drag reduction has often been described for water on superhydrophobic surfaces. A stable plastron is the basis of this effect. Since the 1D-SNF coating shows a plastron not only in water but also in non-polar solvents, reduction of viscous drag can be expected in both types of solvents. However, for 1D-SNF-coated surfaces, no such study has been published yet. More investigations on self-cleaning and drag reduction seem worthwhile.

Other potential applications aside from the prominent wetting properties of 1D-SNF seem to be sidelined up to now. An important basis for any application is the possibility to introduce further chemical functionalities into the 1D-SNF. Especially, the very high specific surface area of 1D-SNF coatings suggests utilisation for, e.g. filtering, catalysis or chromatography. One could also consider a composite phase comprised of 1D-SNF and a matrix material providing useful mechanical, thermal, optical or electrical properties.

8.5. Silicone chemistry

One-dimensional silicone nanostructures can be formed using quite different chemical approaches: growth onto surfaces in the vapour phase or in a solvent and growth of 1D-SNF in a solution catalysed by gold nanoparticles. The organic residues can vary chemically and sterically, e.g. from vinyl to octadecyl. Despite this chemical variability, the resulting one-dimensional silicone nanostructures are always quite similar. This raises the question whether the one dimensionality on the nanoscale might emerge as a more fundamental but yet undiscovered structural principle of polysiloxanes in general. In addition, the question arises whether more complex nanostructures of higher dimensionality may exist.

In view of the widespread use of silicones in the macroscopic world for ~60 years on one hand and the comparably recent discovery of 1D-SNF on the other, the potential applications of 1D-SNF with respect to the specific use of the silicone material supposedly have not been conceived at all.

9. References

[1] Kipping FS, Lloyd LL, J Chem Soc, Trans, 1901; 79: 449.

[2] Rochow EG: Preparation of organosilicon halides, US2380995.

[3] Rochow EG: Silicon and Silicones. Springer; 1987.

[4] Falbe J, Regitz M (editors), Römpp-Lexikon Chemie, Vol. 5. Thieme; 1996-1999.

[5] Cekada J, Weyenberg DR: Colloidal Silsesquioxanes and Methods for Making Same, US3433780.

[6] Artus GRJ, Jung S, Zimmermann J, Seeger S: Superhydrophobic Coating, EP20030405455, WO2004113456.

[7] Gao L, McCarthy TJ, J Am Chem Soc, 2006; 128: 9052.

[8] Artus GRJ, Jung S, Zimmermann J, Gautschi HP, Marquardt K, Seeger S, Adv Mater, 2006; 18: 2758.

[9] Gao LC, McCarthy TJ, Langmuir, 2008; 24: 362.

[10] Rollings DE, Tsoi S, Sit JC, Veinot JGC, Langmuir, 2007; 23: 5275.

[11] Chen R, Zhang X, Su Z, Gong R, Ge X, Zhang H, Wang C, J Phys Chem C, 2009; 113: 8350.

[12] Khoo HS, Tseng F, Nanotechnology, 2008; 19: 345603.

[13] Shirgholami MA, Shateri Khalil-Abad M, Khajavi R, Yazdanshenas ME, J Colloid Interface Sci, 2011; 359: 530.

[14] Zimmermann J, Reifler FA, Fortunato G, Gerhardt L, Seeger S, Adv Funct Mater, 2008; 18: 3662.

[15] Jin M, Wang J, Hao Y, Liao M, Zhao Y, Polym Chem, 2011; 2: 1658.

[16] Rollings DE, Veinot JGC, Langmuir, 2008; 24: 13653.

[17] Gao L, McCarthy TJ, Langmuir, 2007; 23: 9125.

[18] Zimmermann J, Artus GRJ, Seeger S, Appl Surf Sci, 2007; 253: 5972.

[19] Zimmermann J, Reifler FA, Schrade U, Artus GRJ, Seeger S, Colloids Surf, A: Physicochem Eng Aspects, 2007; 302: 234.

[20] Zimmermann J, Seeger S, Reifler FA, Text Res J, 2009; 79: 1565.

[21] Artus GRJ, Seeger S, Ind Eng Chem Res, 2012; 51: 2631.

[22] Veinot JGC, Rollings DE, Tsoi S, Sit J: Substrates Coated with Organosiloxane Nanofibers, Methods for their Preparation, Uses and Reactions thereof, US20080311337.

[23] McCarthy TJ, Gao L: Fibrillar, nanotextured coating and method for its manufacture, US20070135007.

[24] Zhang J, Seeger S, Angew Chem Int Ed, 2011; 50: 6652.

[25] Lorenscheit J, Kurth J: Dichtungsanordnung, DE102010019945.

[26] Kurth J, Lorenscheit J: Dichtungsanordnung, DE102009013969.

[27] Schulz I, Haag C: Lagerkäfig und Lagerkäfigsegment, EP2604877.

[28] Wong JXH, Asanuma H, Yu H, Thin Solid Films, 2012: 159.

[29] Hua Z, Yang J, Wang T, Liu G, Zhang G, Langmuir, 2013; 29: 10307.

[30] Shirgholami MA, Shateri-Khalilabad M, Yazdanshenas ME, Text Res J, 2013; 83: 100.

[31] Hölzer J, Midasch O, Rauchfuss K, Kraft M, Reupert R, Angerer J, Kleeschulte P, Marschall N, Wilhelm M, Environ Health Perspect, 2008; 116: 651.

[32] Fromme H, Tittlemier SA, Völkel W, Wilhelm M, Twardella D, Int J Hyg Environ Health, 2009; 212: 239.

[33] Shirtcliffe NJ, McHale G, Newton MI, Perry CC, Pyatt FB, Appl Phys Lett, 2006; 89: 104106.

[34] Artus GR, Zimmermann J, Reifler FA, Brewer SA, Seeger S, Appl Surf Sci, 2012; 258: 3835.

[35] Zimmermann J, Rabe M, Artus GRJ, Seeger S, Soft Matter, 2008; 4: 450.

[36] Stojanovic A, Artus GRJ, Seeger S, Nano Res, 2010; 3: 889.

[37] Khoo HS, Tseng F, Appl Phys Lett, 2009; 95: 63108.

[38] Zimmermann J: Silicone Nanofilaments as Functional Coatings: Properties, Applications and Modifications; PhD Thesis, University of Zurich; 2008.

[39] Zimmermann J, Artus GRJ, Seeger S, J Adhes Sci Technol, 2008; 22: 251.

[40] Zhang J, Seeger S, Adv Funct Mater, 2011; 21: 4699.

[41] Zimmermann J, Rabe M, Verdes D, Seeger S, Langmuir, 2008; 24: 1053.

[42] Iwasaki Y, Omichi Y, Iwata R, Langmuir, 2008; 24: 8427.

[43] Meseck GR, Kontic R, Patzke GR, Seeger S, Adv Funct Mater, 2012; 22: 4433.

[44] Xia YN, Yang PD, Sun YG, Wu YY, Mayers B, Gates B, Yin YD, Kim F, Yan YQ, Adv Mater, 2003; 15: 353.

[45] Anish KM, Jung S, Ji T, Sensors, 2011; 11: 5087.

[46] Jiang L, Dong H, Hu W, Soft Matter, 2011; 7: 1615.

[47] Kuchibhatla SVNT, Karakoti AS, Bera D, Seal S, Prog Mater Sci, 2007; 52: 699.

[48] Lu W, Lieber CM, J Phys D: Appl Phys, 2006; 39: R387.

[49] Qu Y, Duan X, J Mater Chem, 2012; 22: 16171.

[50] De Volder M, Hart AJ, Angew Chem Int Ed, 2013; 52: 2412.

[51] Wang X, Li Y, Inorg Chem, 2006; 45: 7522.

[52] Rao CNR, Deepak FL, Gundiah G, Govindaraj A, Prog Solid State Chem, 2003; 31: 5.

[53] Chojnowski J, Cypryk M. In Jones RG, Ando W, Chojnowski J (editors), Silicon-Containing Polymers. Kluwer Academic Publishers; 2000.

[54] Baney RH, Cao X. In Jones RG, Ando W, Chojnowski J (editors), Silicon-Containing Polymers. Kluwer Academic Publishers; 2000.

[55] Shateri-Khalilabad M, Yazdanshenas ME, Cellulose (Dordrecht, Neth), 2013; 20: 963.

[56] Stojanovic A, Olveira S, Fischer M, Seeger S, Chem Mater, 2013; 25: 2787.

[57] Zhang J, Seeger S, ChemPhysChem, 2013; 14: 1646.

[58] Gao L, McCarthy TJ, Langmuir, 2006; 22: 2966.

[59] Verho T, Korhonen JT, Sainiemi L, Jokinen V, Bower C, Franze K, Franssila S, Andrew P, Ikkala O, Ras RHA, Proc Natl Acad Sci U S A, 2012; 109: 10210.

[60] Timonen JVI, Latikka M, Leibler L, Ras RHA, Ikkala O, Science, 2013; 341: 253.

[61] Korhonen JT, Huhtamäki T, Ikkala O, Ras RHA, Langmuir, 2013; 29: 3858.

[62] Timonen JV, Latikka M, Ikkala O, Ras RH, Nat Commun, 2013; 4.

[63] Nouri NM, Sekhavat S, Bayani Ahangar S, Faal Nazari N, J Dispersion Sci Technol, 2012; 33: 771.

[64] Wong JXH, Yu H, J Chem Educ, 2013; 90: 1203.

[65] Góral M, J Phys Chem Ref Data, 2004; 33: 1159.

[66] Mączyński A, Wiśniewska-Gocłowska B, Góral M, J Phys Chem Ref Data, 2004; 33: 549.

[67] Patnode WI: Method of Rendering Materials Water Repellent, US2306222.

[68] Norton FJ: Waterproofing treatment of materials, US2412470.

[69] Prasad BLV, Stoeva SI, Sorensen CM, Zaikovski V, Klabunde KJ, J Am Chem Soc, 2003; 125: 10488.

[70] Goyal A, Kumar A, Ajayan PM, Chem Commun, 2010; 46: 964.

[71] Guendouzi ME, Dinane A, Mounir A, J Chem Thermodyn, 2001; 33: 1059.

[72] Vanýsek P. In Lide DR (editor), CRC Handbook of Chemistry and Physics, 85th edition. CRC Press LLC; 2004.

[73] Ulman A, Chem Rev, 1996; 96: 1533.

[74] Iler RK: The chemistry of silica. Wiley; 1979.

[75] Plueddemann EP. In Leyden DE, Collins WT (editors), Silylated surfaces. Gordon and Breach; 1980.

[76] Quéré D, Ann Rev Mater Res, 2008; 38: 71.

[77] Jenkins A, Chambers G, Ind Eng Chem, 1954; 46: 2367.

[78] Sonntag D, Z Meteorol, 1990; 40: 340.

[79] Fakes DW, Davies MC, Brown A, Newton JM, Surf Interface Anal, 1988; 13: 233.

[80] Coulson SR, Woodward IS, Badyal JPS, Brewer SA, Willis C, Chem Mater, 2000; 12: 2031.

[81] Cassie ABD, Baxter S, Trans Faraday Soc, 1944; 40: 546.

[82] Bhushan B, Jung YC, Prog Mater Sci, 2011; 56: 1.

[83] Chen W, Fadeev AY, Hsieh MC, Öner D, Youngblood J, McCarthy TJ, Langmuir, 1999; 15: 3395.

[84] Fadeev AY, McCarthy TJ, Langmuir, 1999; 15: 3759.

[85] Extrand CW, Moon SI, Langmuir, 2010; 26: 17090.

[86] Srinivasan S, McKinley GH, Cohen RE, Langmuir, 2011; 27: 13582.

[87] Quéré D, Rep Prog Phys, 2005; 68: 2495.

[88] Gao L, McCarthy TJ, J Am Chem Soc, 2007; 129: 3804.

[89] Dorrer C, Rühe J, Soft Matter, 2009; 5: 51.

[90] Barthlott W, Neinhuis C, Planta, 1997; 202: 1.

[91] Ganesh VA, Raut HK, Nair AS, Ramakrishna S, J Mater Chem, 2011; 21: 16304.

[92] Asanuma H, Noguchi H, Uosaki K, Yu H, J Phys Chem C, 2009; 113: 21155.

[93] International Organization for Standardization: Textiles - Oil repellency - Hydrocarbon resistance test,ISO 14419, Geneva; 1998.

[94] Parker AR, Lawrence CR, Nature, 2001; 414: 33.

[95] Ruckstuhl T, Rankl M, Seeger S, Biosens Bioelectron, 2003; 18: 1193.

[96] Yuan J, Kimitsuka N, Jin R, ACS Appl Mater Interfaces, 2013; 5: 3126.

[97] Cha JN, Shimizu K, Zhou Y, Christiansen SC, Chmelka BF, Stucky GD, Morse DE, Proc Natl Acad Sci U S A, 1999; 96: 361.

[98] Jin M, Wang J, Yao X, Liao M, Zhao Y, Jiang L, Adv Mater, 2011; 23: 2861.

[99] Jin M, Li S, Wang J, Liao M, Zhao Y, Appl Surf Sci, 2012; 258: 7552.

[100] Kanamori K, Aizawa M, Nakanishi K, Hanada T, Adv Mater, 2007; 19: 1589.

[101] Kanamori K, J Ceram Soc Jpn, 2011; 119: 16.

[102] Li S, Xie H, Zhang S, Wang X, Chem Commun, 2007: 4857.

[103] Li S, Zhang S, Wang X, Langmuir, 2008; 24: 5585.

[104] Zhu Q, Chen N, Tao F, Pan Q, J Mater Chem, 2012; 22: 15894.

[105] Park Y, Ahn Y, Bull Korean Chem Soc, 2011; 32: 4063.

[106] Yan J, Yu J, Zhang W, Li Y, Yang X, Li A, Yang X, Wang W, Wang J, J Mater Sci, 2012; 47: 4159.

[107] Bamoharram FF, Heravi MM, Saneinezhad S, Ayati A, Prog Org Coat, 2013; 76: 384.